

Tucker (personal copy)

NUWC TP 8



n u w c

GAS AND BUBBLE PRODUCTION BY SIPHONOPHORES

By G.V. Pickwell

Marine Environment Division
San Diego, California

September 1967

THE PROBLEM

Investigate and report on the factors in the marine biological environment that pertain to underwater sound; identify and study organisms affecting sound attenuation, scattering, and reflection. Specifically, determine the metabolic capability of siphonophores for bubble production. Determine sizes of voluntarily produced bubbles, their possible resonant frequencies at various depths and their rates of production.

RESULTS

1. Gas-filled siphonophore floats have been studied and photographed in the act of expelling bubbles containing nearly 80 percent carbon monoxide.
2. Resonant frequencies corresponding to the range in measured sizes of voluntarily expelled bubbles, assuming the dimensions to be comparable at depth, are approximately 12 to 58 kc/s at 100 meters (55 fathoms), and 24 to 111 kc/s at 400 meters (220 fathoms), according to existing theory.
3. Maximum rates of bubble production observed were as high as 4 bubbles in 2 minutes or about 30 seconds per bubble.
4. Rate of carbon monoxide production associated with bubble expulsion reached maxima of 115 and $277 \mu\text{l}/\text{mg}$ of gas gland tissue/hr at 20°C , biochemical substrate for gas production being added in the latter case.
5. Oxygen consumption was generally elevated at higher rates of carbon monoxide secretion.
6. Measured volumes of the floats of *Nanomia bijuga* varied from 0.25 mm^3 to 4.92 mm^3 with a single maximum at 12.56 mm^3 , considerably extending the previously observed range. According to the latest theory, these might resonate at 27, 13, and 7 kc/s at

100 meters (55 fathoms) respectively, and at 50, 24, and 13 kc/s at 400 meters (220 fathoms), respectively.

7. Observations of siphonophores from the DEEPSTAR 4000 submersible vehicle, at the daytime depth of the deep scattering layer (DSL), have shown their floats to be fully inflated at all times, and presumably excellent potential sound scatterers for particular frequencies and depths at any time of the day or night.

RECOMMENDATIONS

1. Determine the effects of pressure on the bubble-producing capabilities of siphonophore floats.
2. Determine the lifetimes of bubbles released in the sea by siphonophores.
3. Establish a predictive framework for the relative contribution to sound scattering by siphonophores and their released bubbles within the DSL.

CONTENTS

INTRODUCTION . . .	page 9
METHODS AND RESULTS . . .	13
General . . .	13
Carbon Monoxide Production and Oxygen Consumption . . .	14
Syringe Method . . .	14
Diffusion . . .	27
Carbon Available for Gas Production . . .	31
Nonsecretory Oxygen Consumption . . .	32
BUBBLE PRODUCTION . . .	47
ACOUSTIC ASPECTS . . .	55
NUMBERS OF PHYSONECTID SIPHONOPHORES OBSERVED . . .	64
DISCUSSION . . .	68
Oxygen Consumption and Carbon Monoxide Production . . .	68
Acoustics . . .	70
SUMMARY . . .	73
RECOMMENDATIONS . . .	75
APPENDIX A: PROCEDURE FOLLOWED IN SYRINGE RESPIROMETRY AND GAS PRODUCTION EXPERIMENTS . . .	77
APPENDIX B: EXPERIMENTAL ERRORS AND ACCURACY OF MEASUREMENTS . . .	79
APPENDIX C: EXTERNAL PNEUMATOPHORE DIMENSIONS . . .	81
APPENDIX D: DIFFUSION CONDITIONS FOR SYRINGE EXPERIMENTS . . .	83
APPENDIX E: ANALYSES OF THE FLOAT GASES FROM <i>PHYSALIA</i> , AND FROM <i>VELELLA</i> , . . .	87

Contents (Continued)

APPENDIX F: NOTE REGARDING CONFIRMATORY ANALYSES
FOR CARBON MONOXIDE... 91

REFERENCES... 93

TABLES

- 1 Summary of Cruises . . . page 13
- 2 Oxygen Consumption and CO Production by Nanomian Pneumatophores . . . 17, 18
- 3 Weight of Nanomian Gas Glands . . . 20
- 4 Summary of Secretory Quotients . . . 25
- 5 Diffusive Loss of Carbon Monoxide from Pneumatophores . . . 28
- 6 Carbon Monoxide Diffused vs. CO Produced for Selected Pneumatophores . . . 29
- 7 Ratios: CO Production/ CO Diffusion and Surface/ Volume of Pneumatophores . . . 30
- 8 Respiration of *Physalia physalis* . . . 36
- 9 Respiration of *Velella velella* and *Porpita porpita* . . . 37
- 10 Respiration of Individual Floats of *Nanomia bijuga* . . . 40
- 11 Voluntary Bubbles Produced by Nanomian Pneumatophores . . . 45, 46
- 12 Comparative Sizes of Voluntarily Expelled Bubbles . . . 48
- 13 Resonant Frequencies of Voluntarily Expelled Bubbles and of Pneumatophores . . . 57
- 14 Physonectid Siphonophore Catch by Tucker Net . . . 67
- C-1 External Dimensions of Pneumatophores . . . 82
- E-1 Analyses of Float Gases of *Physalia* . . . 88
- E-2 Analyses of Float Gases of *Velella* . . . 89

ILLUSTRATIONS

- 1 Pneumatophores of *Nanomia bijuga* (Delle Chiaje) showing basal gas glands . . . page 11
- 2 *Physalia physalis* L. Adult specimens preserved in formalin . . . 12
- 3 Micropipette with bubble . . . 15
- 4 Rate of CO production vs. rate of oxygen consumption . . . 21
- 5 Flow diagram of experimental categories . . . 22, 23
- 6 Rate of CO production vs rate of O₂ consumption on basis of gas gland only . . . 26
- 7 The Portuguese Man-of-War, *Physalia physalis* L. 33
- 8 The Sail-by-the-Wind, *Velella velella* (L.) . . . 34
- 9 *Porpita porpita* (L.) . . . 35
- 10 Oxygen consumption of *Physalia* . . . 38
- 11 Oxygen consumption of *Velella* . . . 38
- 12 Oxygen consumption of *Porpita* . . . 39
- 13 Respiratory chamber for micrometer respirometer . . . 41
- 14-16 Oxygen consumption of *Nanomia* . . . 42-44
- 17 Stages in the production of a single bubble . . . 49
- 18 Bubble production by float and in gas gland . . . 50
- 19 Partially expelled bubbles "frozen" by magnesium sulfate . . . 52
- 20 Pneumatophore volume vs. volume of extruded bubbles . . . 53
- 21 Total voluntary bubbles vs. bubble volume . . . 54
- 22 Photos of physonectid siphonophores taken at the depths of the DSL . . . 56
- 23 Ratio of resonant frequencies to ratio of axes of a spheroid . . . 62
- 24 Numbers of physonectid siphonophores observed during three dives in DEEPSTAR 4000 . . . 65
- D1 Hypothetical curves showing possible modes of diffusion in syringe experiments . . . 84, 85

INTRODUCTION

The deep scattering layer (DSL) has been under investigation for the past 25 years since the first systematic observations were undertaken by U.S. Navy scientists and investigators of the University of California Division of War Research.¹

Johnson² first suggested the biological nature of the DSL, while Dietz³ demonstrated the ubiquitous occurrence of this phenomenon in the Pacific. Raitt⁴ discussed the scattering cross section of individual scatterers and pointed out that resonant scattering from small gas bubbles could give values which would be considerably larger than the physical cross section. This feature of resonant bubbles had also been discussed earlier in connection with sound scattering in the sea.¹

The gas enclosure or resonant-bubble theory was developed further in relation to fish swim bladders simultaneously by Marshall⁵ and Tucker.⁶ Both authors demonstrated the occurrence of fishes possessing swim bladders at known daytime depths of the DSL. This aspect was further pursued by Hersey and Backus⁷ when they showed that peaks of resonant frequency of sound scattered by the DSL shifted during vertical migration of the scattering layer. The recorded shift was very nearly proportional to the first power of the depth and was interpreted to indicate gas enclosures, probably fish swim bladders, undergoing passive expansion and contraction with changing hydrostatic pressure during vertical migration. These authors, together with J. Hellwig,⁸ later demonstrated the existence of resonant scattering peaks some of which shifted as the 5/6th power and others as the 1/2 power of the depth. The former case was attributed to fish swim bladders responding passively to pressure changes, whereas the latter case was taken to imply fish swim bladders maintained at constant volume.

Subsequently, Barham,^{9, 10} during a series of dives in the bathyscaphe TRIESTE I, made the surprising discovery that siphonophores, especially of the float-bearing suborder, Physonectae, were consistently present at the precise depths of the DSL in comparatively large concentrations, but were less

¹ Superscript numbers identify references listed at end of report.

concentrated or absent at other depths. Batzler and Barham¹¹ demonstrated an unusually high scattering coefficient (the fraction of sound scattered per unit of vertical travel in the water column) from depths where physonectid siphonophores were present in great abundance to the exclusion of virtually all other potential sound scatterers.

It appears that siphonophores had been overlooked as sound scatterers up to this time because of their fragility, and the poor and fragmented condition in which they were taken in nets hauled through the DSL. It soon became clear that most of the assumptions made concerning fishes with swim bladders as effective acoustic targets, and much of the evidence which had been collected could be applied equally as well to siphonophores bearing gas-filled floats or pneumatophores.

Additional observations made by Barham¹² using the Cousteau diving saucer and recently the Westinghouse DR/V DEEPSTAR 4000¹³⁻¹⁵ have conclusively placed physonect siphonophores with certain fishes as the primary acoustic targets within the DSL in the areas where observed and at the sonar frequencies employed. In fact, it now appears that scattering from some sub-layers within multicomponent scattering layers may be due exclusively to siphonophores of the float-bearing physonect type.¹²

Further investigation into the physiology and gas dynamics of these intriguing organisms revealed the gas within their minute floats to be nearly pure carbon monoxide¹⁶ which, it is presumed, arises via an enzymatic system housed within the cells of the basal, goblet-shaped gas gland (fig. 1). This has been shown to be the case in the surface-dwelling siphonophore, the Portuguese Man-of-War, *Physalia*¹⁷ (fig. 2). Additional investigations¹⁸ have shed some light on the range of float dimensions which can be expected from a population of these physonect siphonophores, particularly the most abundant species in San Diego waters, *Nanomia bijuga* (Delle Chiaje). The range observed was approximately 0.5 to 2.5 mm³. In addition, some first measurements on the rate of oxygen consumption by these creatures were made and these related to the energy requirements of the physical component of the work performed to counter hydrostatic pressures at normal DSL depth.¹⁸ Further observations provided data on rate of diffusional loss of CO across the pneumatophore walls and these in turn permitted estimates of the gas secretion necessary simply to counter this diffusive loss. Rates so determined were

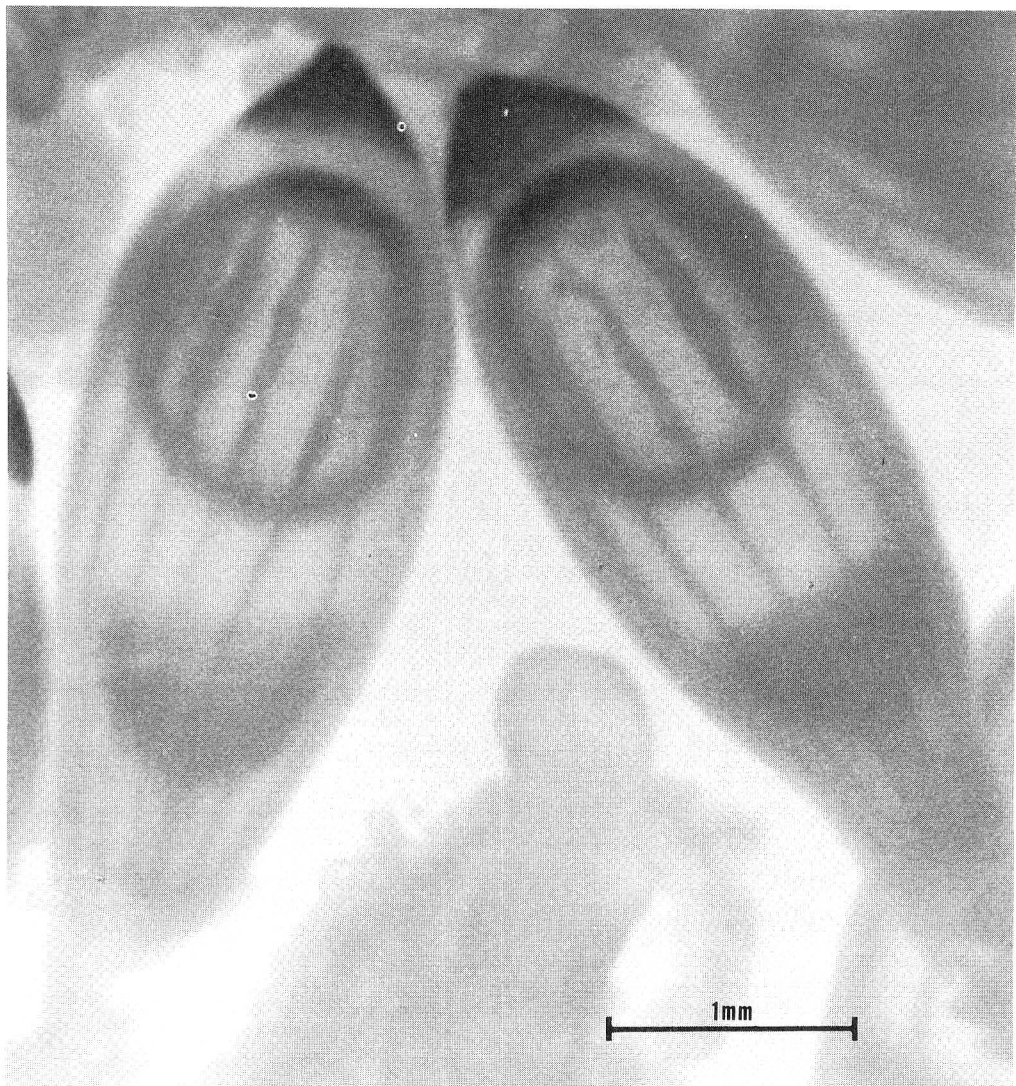


Figure 1. Pneumatophore specimens of *Nanomia bijuga* (Delle Chiaje) broken off from the remainder of the colony during net collection. The cup-shaped gas glands are clearly visible through the walls of these preserved individuals.

related to known diffusion rates of gases across animal tissues and lent support to the hypothesis that the diffusion barrier in the walls of the pneumatophore is probably chiton as apparently is the case in *Physalia*¹⁹. Included in the above study¹⁸ was a single experiment that indicated the actual measured rate of CO production could be at least great enough to counter the measured diffusive loss. This suggested the reasonable idea that the gas-secreting system may actually run at some minimal rate just sufficient to counter loss by diffusion even though the float is fully inflated. The observation

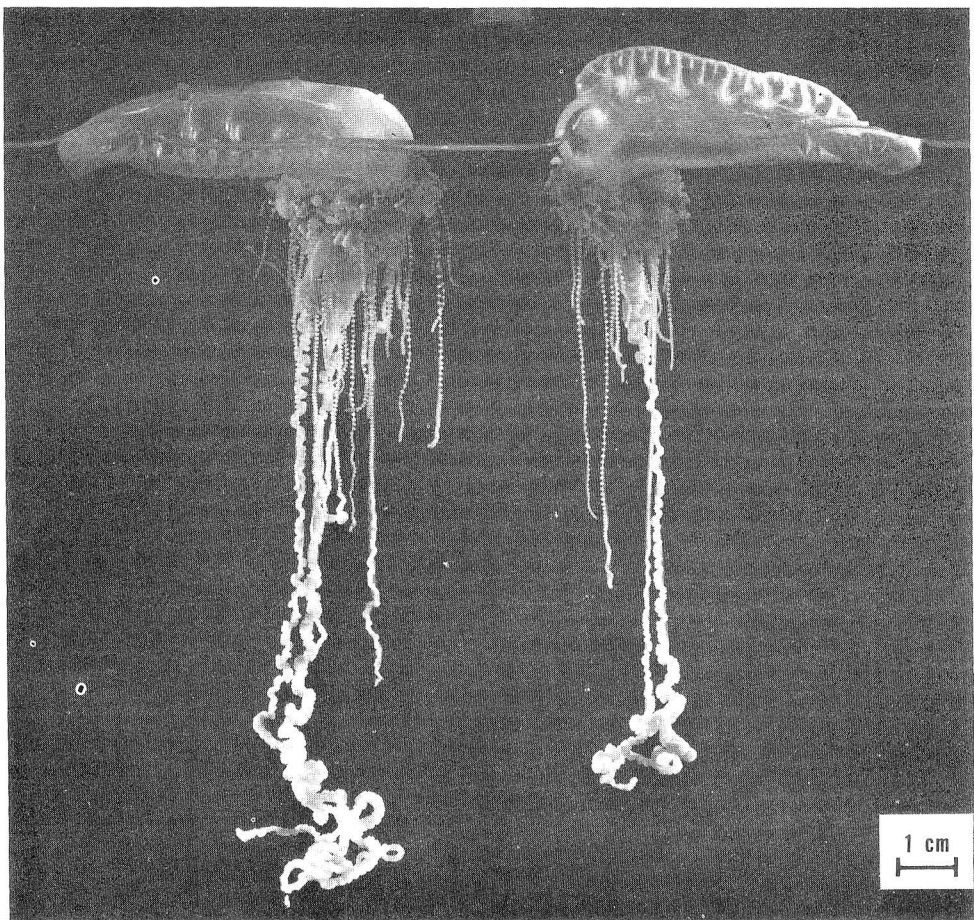


Figure 2. Preserved adult specimens of the Portuguese Man-of-War, *Physalia physalis* L. collected in the East China Sea.

was also made that upward migration would produce, through a pore present at the float apex, a stream of bubbles, of still to be determined size and frequency, from the continuously expanding gases within the siphonophore float, a suggestion also made earlier.^{9, 16}

In the present report a more comprehensive study has been made of the respiratory exchange by the isolated pneumatophore of *Nanomia bijuga* in comparison with nonsecreting, surface-dwelling siphonophores. Rates of production of carbon monoxide have been carefully assessed and direct observations of bubble-production rates are reported and discussed. Actual measurement and collection of spontaneously expelled bubbles, together with *in situ* observations of siphonophores from a deep submersible

are reported. Resonant frequencies covering the range of pneumatophore size as well as the range in size of expelled bubbles after adjustment to various depths are listed and discussed.

METHODS AND RESULTS

General

The data to be presented here were obtained at sea on the cruises summarized in table 1. *Nanomians* were captured using a 2-meter-square Tucker net^{6, 20} hauled through the DSL at 4 to 5

TABLE 1. SUMMARY OF CRUISES FROM WHICH DATA WERE OBTAINED

Ship	Date	Cruise Designation	Location	Object of Study; Methods Employed
USS MARYSVILLE (EPCER 857)	8/10-12/65	Operation Siphonophore IV	32°18'W 117°28'W	<i>Nanomia</i> ; microrespirometry
USS REXBURG (EPCER 855)	9/14-17/65	Operation Siphonophore V	32°18'N 117°28'W	<i>Nanomia</i> ; bubble production
USS REXBERG	8/1-4/66	Operation Siphonophore IX	32°35'N 117°43'W	<i>Nanomia</i> ; bubble photos
USS REXBURG	8/29-9/1/66	Operation Siphonophore X	32°08'N 32°08'N 117°59'W, 117°49'W	<i>Nanomia</i> ; bubble photos
USS REXBURG	10/3-7/66	Operation Siphonophore XI	32°34'N 32°34'N 118°10'W, 117°59'W	<i>Nanomia</i> ; syringe respiration and gas production
USNS CHARLES H. DAVIS (T-AGOR 5)	5/66-7/66	FASOR II	S. China Sea, E. China Sea	<i>Physalia</i> , <i>Veella</i> , <i>Porpita</i> ; microrespirometry
DR/V DEEPSTAR 400 aboard M/V BURCH TIDE	10/21/66	Dive 159*	32°31.5'N 117°27.1'W	DSL; direct observations, notes, <i>in situ</i> photos
DR/V DEEPSTAR	11/10/66	Dive 170*	32°31.5'N 117°27.1'W	DSL; direct observations, notes, photos
DR/V DEEPSTAR	11/30-12/ 1/66	Dives 182, 183, 184*	32°48'N 32°38'N 117°27'W, 117°35'W	DSL; direct observations, notes, photos

*Dive 159: pilot, Church - observers, Barham, Pickwell; Dive 170: pilot, Thompson - observers, Davies, Pickwell; Dives 182, 183, 184: pilots, Thompson, Bradley, Church, respectively - observers, Adams, Pickwell.

knots for periods of 1/2 to 3 hours. Surface siphonophores were collected using dip-nets and buckets lowered from the ship's side while hove-to.

Because the delicate nanomians do not usually rise completely to the surface in San Diego waters where they might be collected intact, it was necessary to perform all experiments on the severed floats alone. These structures are easily identified among the other organisms and debris in the cod-end bucket after a net haul because they float to the surface of the bucket where the bright red pigmentation at the tip of the pneumatophore is readily seen. The floats are then carefully removed with forceps and placed in a dish for sorting. Those not used immediately in experiments were placed in a refrigerator at 6 to 7°C until needed.

The validity of data obtained from these separate individuals, rather than from the intact colony, was verified in a previous report,¹⁸ using intact specimens of another suborder and is further substantiated by data presented below from intact, surface-dwelling siphonophores and related forms.

Respirometry and gas-secretion experiments, analyses, and photographic work on nanomian floats were performed in an instrument van equipped for these purposes and secured to the deck of the ship. Experiments on surface siphonophores were conducted in a shipboard temperature-regulated, photographic darkroom.

Carbon Monoxide Production And Oxygen Consumption

SYRINGE METHOD

The most convenient method for following O₂ uptake and CO production involved the use of 1-cc tuberculin glass hypodermic syringes. These were completely filled with filtered seawater (Schleicher and Schull filter No. 576), the pneumatophore specimen added together with a drop of mercury for stirring, and then carefully sealed without entrapped air. Blank controls were run simultaneously in syringes containing only seawater and a mercury drop. Temperature control was maintained by placing the syringes

in a 1.5 cu ft refrigerator consistent to $\pm 0.5^\circ$ for the subambient runs at 9°C , or in a water bath thermoregulated to $\pm 0.3^\circ\text{C}$ by a large-capacity, refrigerated, constant-temperature circulator bucked against a circulating heater for runs at 11° C and higher. Occasional rotation and end-to-end tilting of the syringes kept the contents stirred by the mercury drop. The *in situ* temperature range for *Nanomia* as observed from DR/V DEEPSTAR and also recorded in the literature²¹ drops from near-surface values of 12° C to about 6.5° C at the lower depths of the DSL (see fig. 24, in the section entitled "Numbers of Physonectid Siphonophores Observed").

At the start of a run a sample of the seawater stock was analyzed for dissolved oxygen by the method of Scholander *et al.*²² After a period of time the syringes were removed one at a time from the refrigerator or water bath and the contents analyzed according to the procedure summarized in Appendix A.* Analyses of the small quantities of gas obtained from the float were performed in the Scholander water analyzer²² or in a micropipette. When employing the micropipette, the volume of the gas bubbles after absorption of CO_2 , then O_2 and finally CO , by suitable reagents, was evaluated using an ocular micrometer in a dissecting scope at $12 \times$ (fig. 3). Volume of the gas phase within the pneumatophore was calculated as a prolate spheroid. This has

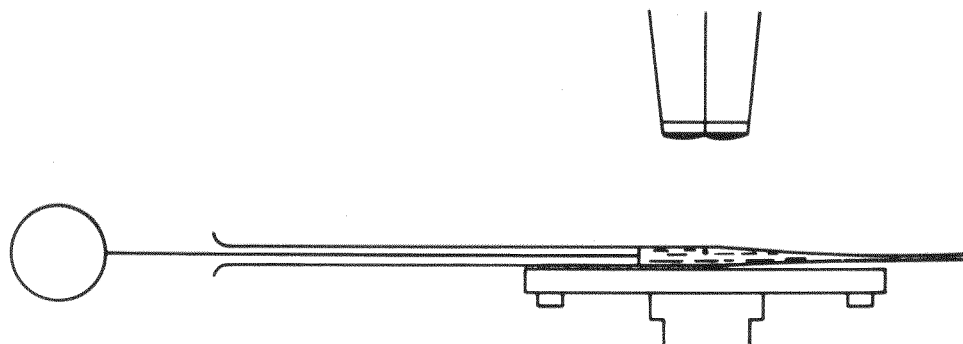


Figure 3. Micropipette with bubble under dissecting microscope. Bubbles were analyzed in pipettes by addition of suitable absorbers. Measures of bubble diameter were taken with an ocular micrometer after each successive absorption for CO_2 , O_2 , and CO .

* Additional discussion of the errors involved in this method is given in Appendix B.

been shown to be the most reliable means of obtaining volume estimates when the total gas could not be expelled, collected, and measured.¹⁸

In the syringe method CO_2 will accumulate while O_2 declines, and CO will diffuse out of the float and build up in some concentration when there is secretion or when the initial percentage in the float is high. Although it is obvious that no CO poisoning occurs within the float, it has not been shown whether external tissues are susceptible to CO poisoning. In addition, increased CO_2 may increase respiration, thereby accelerating the decline in oxygen. Dependence of respiratory rate on oxygen tension has been demonstrated in a number of invertebrate animals²³ but the decline in oxygen consumption with low partial pressure of oxygen (pO_2) generally appears at comparatively low levels and is not evident in the present study. In an experiment showing a large decline in dissolved O_2 , the resultant CO_2 , although buffered to a considerable extent by the bicarbonate system in the sea water, can cause a drop in pH from about 8.3 to as low as about 7.5. This could have profound effects upon the physiological systems involved but again, as will be shown below, is not demonstrated by data from the syringe experiments.

These data are presented in table 2. To facilitate comparison with subsequent data the respective rates of oxygen consumption and carbon monoxide production, after correction for standard conditions, have been adjusted to 20°C by use of the Van't Hoff equation (here termed 'VH₂₀') assuming a Q_{10} of 2. This equation simply states that for a 10°C rise in temperature within the physiological range of the organism, there will be an increase in a given physiological function of some constant value, in this case 2; that is, a doubling. The Q_{10} of some respiratory processes is about 2.²⁴

In its simplest form the equation may be written

$$\log Q_{10} = \frac{10}{t_2 - t_1} \log \frac{k_2}{k_1} \quad (1)$$

where k_1 and k_2 are the rates of the reaction in question when measured at temperatures t_1 and t_2 , respectively.

By selecting experiments from table 2 having as nearly identical conditions as possible, a Q_{10} for oxygen consumption was determined using one pair of floats without substrate and a second Q_{10}

TABLE 2. OXYGEN CONSUMPTION AND CO PRODUCTION BY
NANOMIAN PNEUMATOPHORES* (Continued on page 18)

	Pneumatophore Blotted Wet Weight (mg) With Stolon / Without Stolon	Volume of Float Gas Phase ** (mm ³)	Float Condition at End of Run†	Medium	Total Experiment Time (hr:min)	Bath or Refrigerator Temp. (°C±0.5)	Avg. O ₂ Consumption for Control (mm ³ /mg/hr) (total wt.)	O ₂ Consumption Corrected for Control (mm ³ /mg/hr) (total wt.)	O ₂ Consumption Readjusted to STPD & VH ₂₀ STPD / VH ₂₀	CO Production in Terms of Total Wt.(mm ³ /mg/hr) Gland = 10% of Float Wt. (mm ³ /mg/hr)	CO Production in Terms of Gland = 10% of Float Wt. (mm ³ /mg/hr)	CO Production, 10% Gas Gland Readjusted to STPD & VH ₂₀ STPD / VH ₂₀	Remarks		
O	1.6	0.4	2.23	Fair	0.05M L-serine in Seawater	23:06	7.5	0.105	0.095	0.225	0.052	2.100	1.896	4.500	
D	0.4	0.3	0.29	Good	Seawater	22:38	6.0	0.012	0.011	0.028	0.024	0.320	0.283	0.746	1 bubble produced; see table 11.
C	3.0	1.2	1.30	Good	Seawater	22:28	7.0	0.011	0.010	0.024	0.031	0.765	0.686	1.691	1 bubble produced; see table 11.
N	2.3	0.4	2.07	Fair	0.05M L-serine in seawater	22:02	7.5	0.003	0.002	0.006	0.005	0.290	0.262	0.623	3 bubbles produced; see table 11.
J	4.4	0.9	3.06	Dead	Seawater	18:25	21.5	0.013	0.012	0.011	0.001	0.066	0.060	0.054	Float degassed by mild vacuum
L	2.1	0.6	1.10	Dead	Seawater	18:24	21.0	0.092	0.083	0.077	0.024	0.850	0.764	0.710	
K	2.0	0.5	1.57	Dead	Seawater	18:20	21.0	0.059	0.053	0.050	0.011	0.420	0.378	0.352	Float degassed
I	3.9	1.3	0.93	Dead	Seawater	16:58	21.5	0.031	0.027	0.026	0.002	0.060	0.054	0.049	Float degassed
G	4.0	1.3	0.74	Fair	Seawater	15:17	8.0	No data			0.029	0.447	0.400	0.928	
H	6.6	2.5	1.60	Good	Seawater	14:05	9.0	0.014	0.012	0.026	0.023	0.597	0.533	1.132	4 bubbles produced; see table 11.
R	1.3	0.4	1.11	Good	0.02M L-serine in seawater	13:40	7.0	0.097	0.088	0.216	0.016	0.520	0.470	1.156	

TABLE 2. (Continued)

Q	2.3	0.9	1.57	Good	0.02M L-serine in seawater	13:15	7.5	No data	0.050	1.270	1.145
F	8.8	3.0	2.89	Good	Seawater	12:49	8.0	0.024	0.021	0.049	0.780
P	3.1	1.2	1.65	Fair	0.02M L-serine in seawater	12:23	7.5	0.089	0.081	0.183	0.040
M	1.3	0.3	0.95	Fair	Seawater	11:37	21.5	0.374	0.337	0.314	0.055
B	3.7	1.5	2.16	Good	Seawater	11:37	7.0	0.129	0.116	0.285	0.039
A	0.5	0.29	Dead	Seawater	8:32	7.0	No data		No data		
U	1.0	0.3	0.66	Fair	0.02M L-serine in seawater	7:09	21.0	0.298	0.269	0.250	0.069
T	0.9	0.2	0.73	Fair	0.02M L-serine in seawater	5:21	21.0	0.511	0.462	0.430	0.097
S	0.7	0.3	0.62	Good	0.02M L-serine in Seawater	4:54	21.0	0.464	0.419	0.390	No data

*Determined by syringe method. See Appendix C, Table C-1, for external dimensions of the floats listed in this table.

**Gas phase volume at start of experiment, estimated as a prolate spheroid. All determinations made at 21 to 24°C.

†Condition of float at end of experimental run was arbitrarily assigned to one of three groups on the basis of appearance: "Good," showed typical translucent appearance of float walls seen in fresh-caught specimens, no indication of loss of toxicity by muscles in the float wall, and generally a reddish color of pigment; "Fair," showed some darkening of pigment with some loss of muscle tone resulting in occasional out-pouchings of float wall; "Dead," showed blackened, pigmented area, completely opaque float walls and various indications of loss in muscle tone such as out-pouchings of walls, and constrictions and pinching's in the apical pore areas.

was determined for a pair of floats provided with a substrate for gas production. Thus, using experiments M and B, $Q_{10} = 2.1$; using experiments P and U, $Q_{10} = 2.4$.

Whittenberg¹⁷ determined that excised gas-gland tissue from the surface siphonophore *Physalia*, when incubated with L-serine, produced detectable quantities of CO. Accordingly, some of the nanomian floats in the syringe experiments were provided with this amino acid in concentrations of 0.02M or 0.05M in seawater. Using the same two pairs of floats, the Q_{10} for gas production for both was found to equal 1.8, thus indicating no apparent effect of substrate on the temperature coefficient for gas production. In addition, a measurable quantity of CO above that already present within the float was produced in most experiments. This further supports an earlier hypothesis that pneumatophores continuously produce CO at some "idling" rate in order to counter diffusive loss.¹⁸

Production of CO, however, in most cases, is clearly elevated in the presence of substrate. In addition, rate of O₂ consumption generally increases with CO production as first demonstrated by Pickwell,¹⁸ thus further substantiating the suggestion of Whittenberg¹⁷ that oxygen may be required for CO formation.

On the basis of analysis and direct observation,^{16,25,26} the gas gland in the basal or "funnel" area of the pneumatophore (fig. 1) can be regarded as the sole site of CO production. By carefully dissecting out this delicate, goblet-shaped structure from a series of preserved floats, the gas gland was found to average about 8 percent of the total float weight after removal of all attached stolon (table 3). For convenience, a 10-percent ratio of gas gland to total float was assumed in calculating the rate of gas production per milligram of gas-gland tissue (table 2). Again, these values have been recalculated to VH₂₀ for ease in later comparisons.

The relationship between oxygen consumption and CO production is shown in figure 4. CO production per milligram of gas gland is plotted against oxygen consumption of the entire float and its attached fragment of stolon. The grouping of the points immediately suggests that added substrate does indeed usually enhance CO production, and that oxygen consumption is also correspondingly elevated. However, there are also several floats which apparently possessed enough substrate, presumably already in the

TABLE 3. WEIGHT OF NANOMIAN GAS GLANDS

Float	Weight of Float + Gas Gland* (mg)	Weight of Gas Gland* (mg)	Ratio of Gas Gland Wt. /Float + g.g. Wt. X 100 (%)
I	3.6	0.6	16.7
II	3.9	0.4	10.3
III	4.3	0.2	4.7
IV	3.2	0.3	9.4
V	3.5	0.2	5.7
VI	3.0	0.1	3.3
		Avg.	8.3

*Precise to ± 0.1 mg. All attached stolon removed.

gas gland or in the gastrovascular fluid within the stolon feeding the gas gland, to support CO secretion at elevated rates. Some of these do not appear to have an increased oxygen consumption.

To clarify this apparent anomaly and further quantify these results, the assumption was made that the gas gland is by far the most metabolically active part of the pneumatophore (values presented in the section entitled "Nonsecretory Oxygen Consumption," p. 15, confirm the validity of this assumption). The data for oxygen consumption were then calculated using VH_{20} figures based on a gas gland representing 10 percent of the total float weight (compare table 3). These data were equated against the corresponding data for CO production to give a secretory quotient, or SQ. This is simply the ratio of CO produced to O_2 consumed. This ratio and the resulting SQ are included in figure 5, a diagram drawn to clarify the experimental arrangements.

It is immediately apparent from this figure that the severed floats of *Nanomia* cannot survive long periods at high temperatures. It also appears that a group of floats under nearly identical conditions will not always react in the same way. Thus, although the floats seem to survive for longer periods at low temperatures they do not appear to do as well with added substrate. This suggests a possible osmotic difficulty due to the presence of serine,

• = WITHOUT SUBSTRATE ● = WITH SUBSTRATE CONCENTRATION AS SHOWN.

20°C

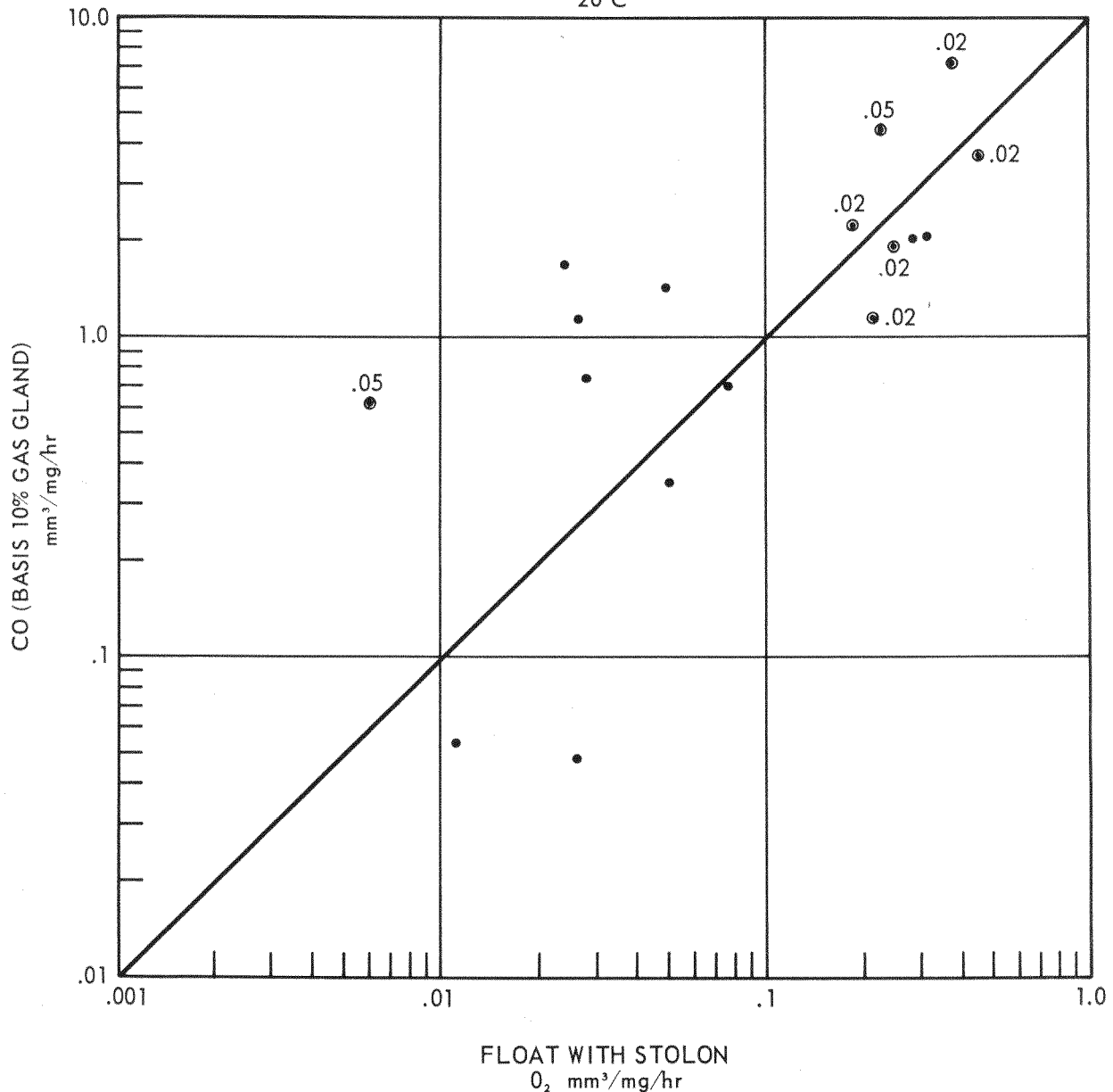


Figure 4. Rate of CO production vs. rate of oxygen consumption. CO is equated on the basis of gas-gland weight estimated as 10% of the weight of float with all attached stolon removed. O_2 is equated here on the basis of total specimen weight. Experiments utilizing 0.02M or 0.05M L-serine are indicated by circled points. The straight line represents 10 CO to 1 O_2 , conditions and units as stated. All values have been adjusted to 20° C by the Van't Hoff equation using $Q_{10} = 2$.

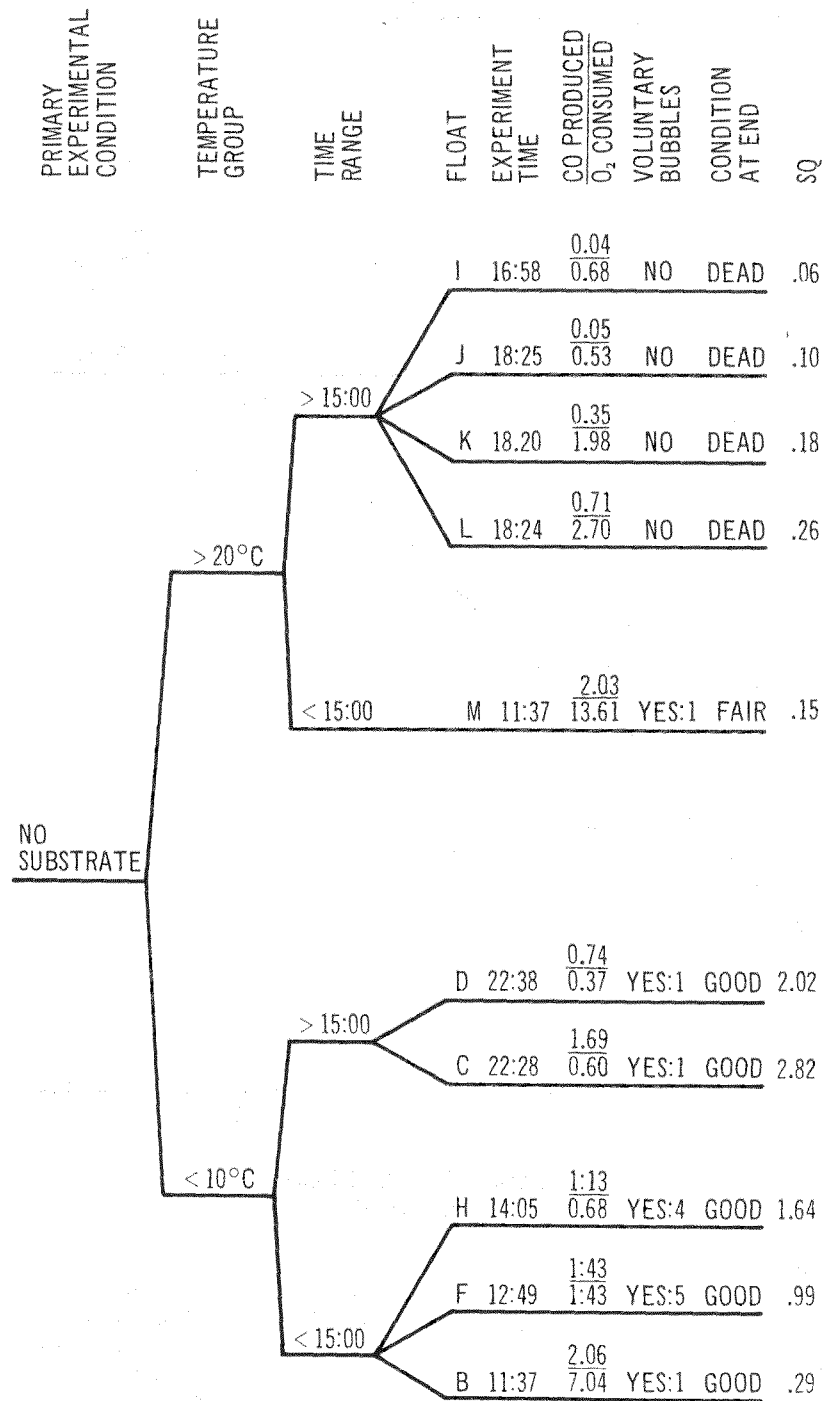


Figure 5. Flow diagram of experimental categories for syringe experiments. Results are equated on the basis of 10% gas gland for both CO and O₂, all adjusted to 20° C. From this ratio the secretory quotient (SQ) is derived.

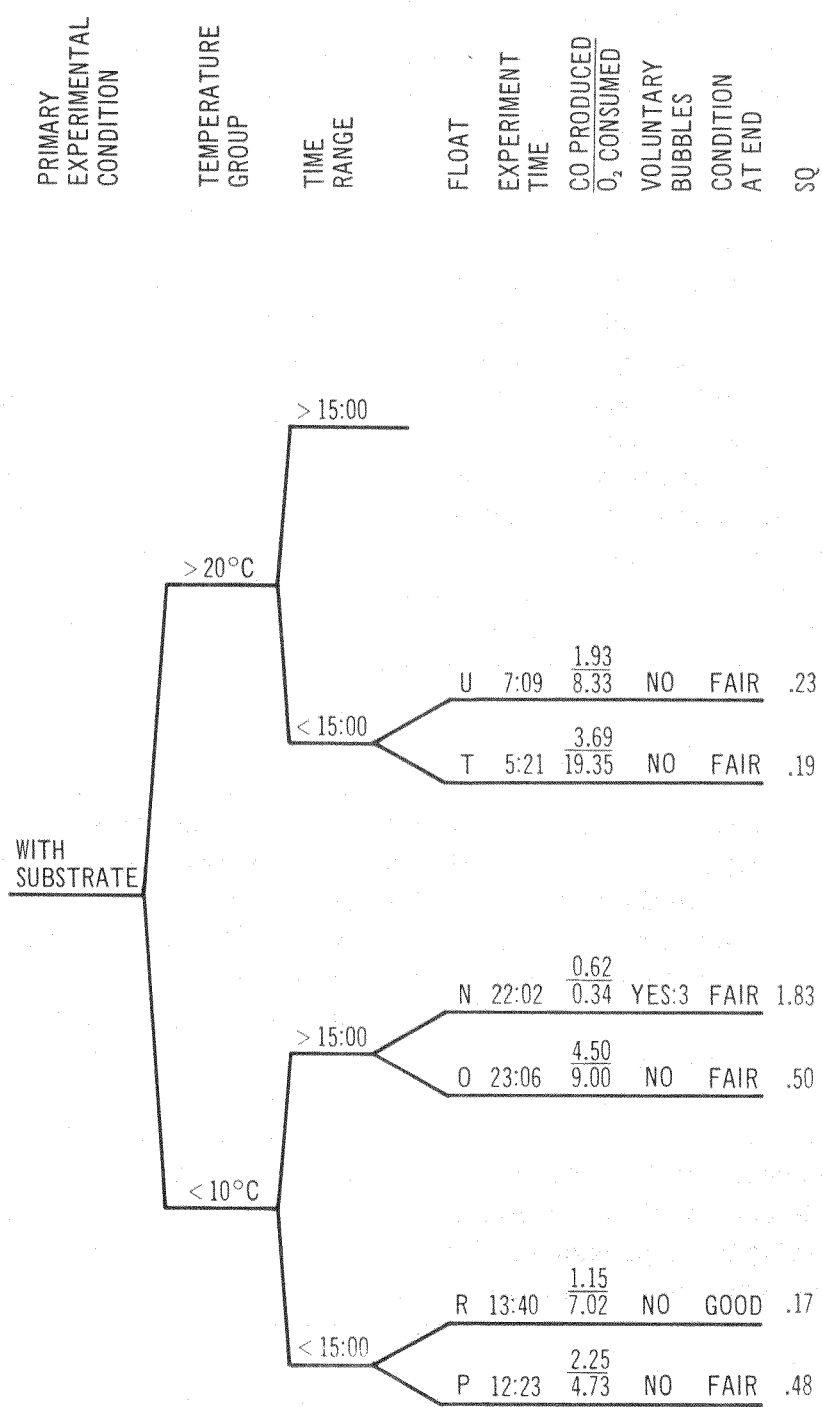


Figure 5 (Continued)

but may also be due to the more rapid consumption of available oxygen. Another possibility may be variability in float condition at the start of the experiment. This last feature is difficult or impossible to assess. No respiratory substrate was added to the syringe seawater, so it seems possible that the apparent acceleration of oxygen consumption with CO production may have exhausted the pneumatophore tissues.

Ignoring those experiments in which the pneumatophores died, the secretory quotients from 12 experiments are summarized in table 4. A plot of CO production versus O₂ consumption on the basis of gas-gland weight is presented in figure 6. From these data, two distinct groups of CO secreting floats emerge. Group I is characterized by relatively low rates of CO production (although high relative to reported values from *Physalia*^{27,28}) and an average SQ close to 2. This may be indicative of the idling or antidiiffusive rate of gas production mentioned earlier, and suggests one molecule of O₂ consumed for each two molecules of CO secreted. Group II, on the other hand, is characterized by more rapid gas production, an average increase of about 2 times, while oxygen consumption correspondingly increased by a factor of some 14 times. The resultant average SQ for Group II suggests three to four oxygen molecules consumed for each CO molecule produced. While further experiments are needed to fully validate these results, one interesting feature to be considered is that some of the additional energy available from the enhanced oxygen consumption might be utilized in the physical work of countering the collapsing effect of hydrostatic pressure at the daytime depths of the DSL. An earlier observation¹⁸ pointed out that the work required to maintain the inflated pneumatophore against these pressures was equal to about half the energy available from the oxygen consumed in one hour at measured rates. Accelerated O₂ consumption might then provide additional energy for the work of countering hydrostatic pressures of 30 to 40 atmospheres, thus enabling the float to reinflate sooner after downward migration, or permit it to more readily resist these pressures if maintaining neutral buoyancy during downward migration. In addition to gas-phase dimensions listed in table 2, see also the external dimensions of the same floats given in Appendix C.

It is possible that the bimodal grouping of the floats in figure 6 is fortuitous and a larger series of experiments might have shown a continuous series with intermediate rates as well.

TABLE 4. SUMMARY OF SECRETORY QUOTIENTS

Float	O ₂ Consumed on a 10% Gas Gland Basis Adjusted to VH ₂₀ (mm ³ /mg/hr)	CO Produced on a 10% Gas Gland Basis Adjusted to VH ₂₀ (mm ³ /mg/hr)	SQ CO/O ₂
Group I	D	0.37	0.75
	C	0.60	1.69
	N*	0.35	0.62
	H	0.69	1.13
	F	1.44	1.43
			Avg. 1.92
Group II	O*	9.00	4.50
	R*	7.02	1.16
	P*	4.73	2.26
	M	13.61	2.04
	B	7.04	2.06
	U*	8.33	1.93
	T*	19.35	3.70
			Avg. 0.29

*Floats marked with an asterisk had added substrate for gas production.

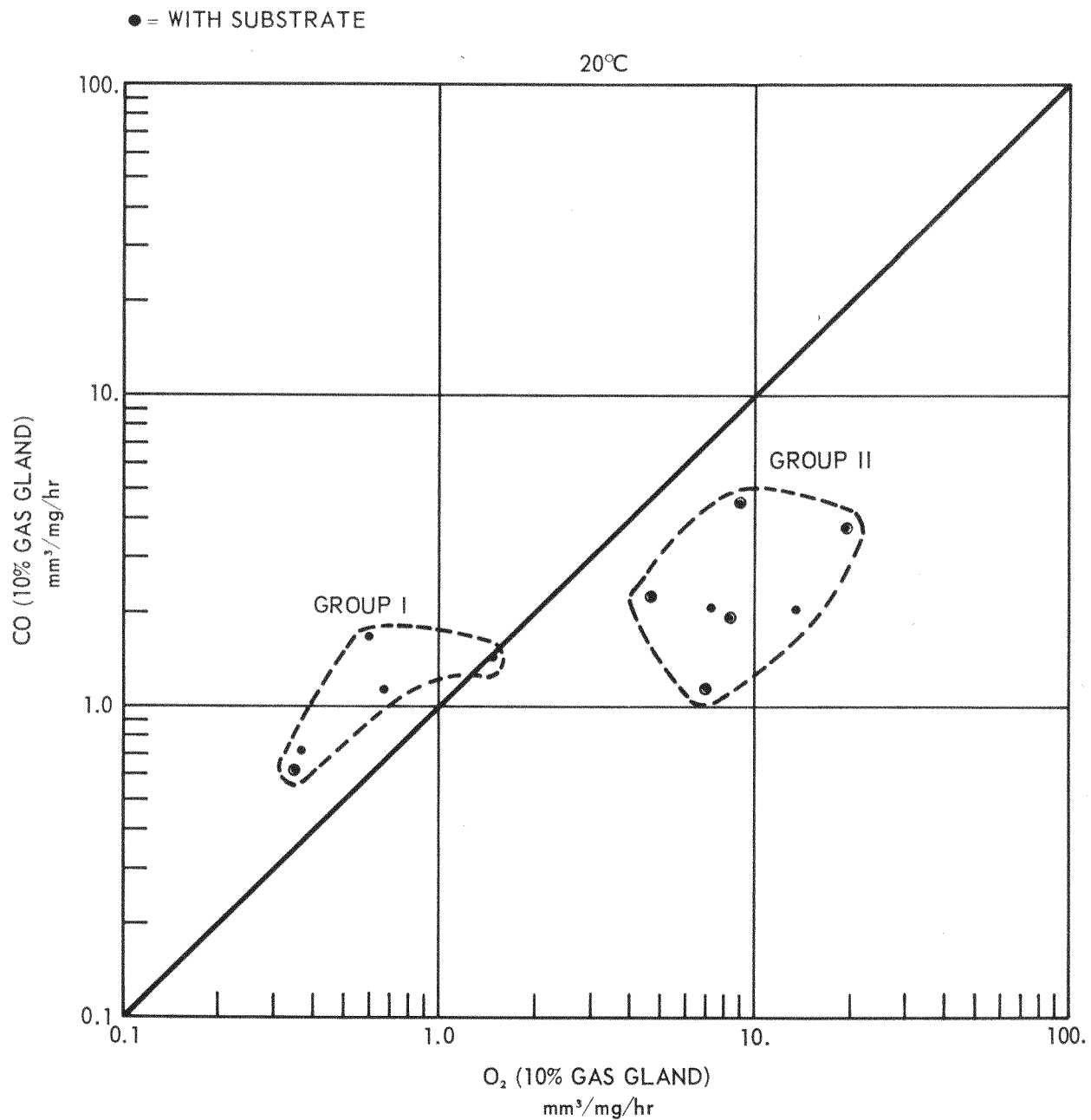


Figure 6. Rate of CO production vs. rate of O_2 consumption. Both rates equated on the basis of gas gland only assuming a weight equal to 10% of float weight without stolon. All values adjusted to 20°C . The straight line represents CO production equal to O_2 consumption.

Diffusion

While the SQ values provide a convenient means of comparing CO production and O₂ consumption they may tend to obscure other relationships. Although CO production, when equated against an average weight of gas-gland tissue, is generally accelerated upon addition of substrate, it is not apparent from these data how this relates to diffusive loss.

The total quantity of CO dissolved in the syringe water was assumed to represent the amount that diffused across the entire float surface when no released bubbles were found in the syringe. Table 5 presents the surface areas of all floats from table 2 calculated as regular prolate spheroids, and the total amounts of diffused CO. The rates per unit area per hour in table 6 encompass those reported previously.¹⁸ Again using the floats employed in SQ groups I and II plus float Q, an interesting feature is shown in table 6 in which total quantities of CO diffused across the float wall are compared with total quantities of gas produced exclusive of expelled bubbles. It is interesting that some floats, particularly most from SQ Group II, did not produce enough gas per hour to counter diffusive loss. This is possible if these pneumatophores performed the greater part of their gas production toward the end of the experimental period.*

Other factors such as temperature, condition of float (a factor related in part to temperature), and possibly the presence of substrate also have a bearing on diffusive loss. Some of the apparent importance of the latter factor is clearly seen in table 7. It appears that any effect resulting from a comparatively unfavorable surface-to-volume ratio is masked by one or more of the factors stated above, particularly temperature, float condition, and diffusion gradient.

The range in diffusion rates is approximately an order of magnitude. This is small considering the extent of experimental conditions and the various factors affecting the individual pneumatophores. Therefore, the idling gas production hypothesis still appears valid. Furthermore, all floats in table 2 and subsequent tables produced gas at some rate however slight. Under pressure the diffusional loss can be expected to rise with the

*A more complete discussion of the factors relating to CO production vs. CO diffusion is presented in Appendix D.

TABLE 5. DIFFUSIVE LOSS OF CARBON MONOXIDE FROM PNEUMATOPHORES

Float	Weight of Pneumato-phore* (mg)	Volume of Gas Phase** (mm ³)	Area of Pneumatophore** (mm ²)	Total Dissolved CO in Syringe (mm ³)	Total Diffusion Time (min)	Diffusive Loss (mm ³ /float/hr)	Diffusion Rate (mm ³ /mm ² /hr)	Remarks
O	0.4	2.23	13.49	1.65	1386	0.065	0.005	
D	0.3	0.29	5.26	0.07	1358	0.003	0.001	
C	1.2	1.30	11.41	0.61	1348	0.025	0.002	
N	0.4	2.07	13.35	2.02	1322	0.083	0.006	
J	0.9	3.06	19.27	0.30	1105	0.014	0.001	Float degassed at start
L	0.6	1.10	9.17	1.38	1104	0.068	0.007	
K	0.5	1.57	10.17	0.38	1100	0.019	0.002	Float degassed at start
I	1.3	0.93	9.56	0.19	1018	0.010	0.001	Float degassed at start
G	1.3	0.74	12.51	1.57	917	0.092	0.007	
H	2.5	1.60	18.37	1.15	845	0.073	0.004	
R	0.4	1.11	9.59	0.96	820	0.064	0.006	
Q	0.9	1.57	11.78	1.30	795	0.089	0.008	
F	3.0	2.89	21.52	1.42	769	0.099	0.005	
P	1.2	1.65	21.86	1.99	743	0.161	0.007	
M	0.3	0.95	10.46	1.69	697	0.132	0.013	
B	1.5	2.16	16.72	1.57	697	0.121	0.007	
U	0.3	0.66	6.90	0.76	429	0.097	0.014	
T	0.2	0.73	6.99	0.88	321	0.149	0.021	

*These are weights of the float only, with all attached stolon removed.

**Calculated as a regular prolate spheroid. All measurements at 21-24°C.

TABLE 6. CARBON MONOXIDE DIFFUSED VS. CO PRODUCED
FOR SELECTED PNEUMATOPHORES

Float	CO Diffused STPD (mm ³ /mm ² /hr)	Total CO Diffused STPD (mm ³ /hr)	Total CO Produced STPD (mm ³ /hr)
D	< 0.001	0.003	0.008
C	0.002	0.025	0.083
H	0.004	0.073	0.135
O*	0.005	0.065	0.074
F	0.005	0.099	0.243
N*	0.006	0.083	0.010
R*	0.007	0.064	0.019
B	0.007	0.121	0.129
P*	0.007	0.161	0.112
Q*	0.008	0.089	0.045
M	0.013	0.132	0.061
U*	0.014	0.097	0.062
T*	0.021	0.149	0.079

*Substrate for gas production added.

TABLE 7. RATIOS: CO PRODUCTION/CO DIFFUSION AND SURFACE/VOLUME OF PNEUMATOPHORES

Float	Total Experiment Time (min)	CO Production >Diffusion (CO Prod.) CO Diff.	CO Production <Diffusion (CO Diff.) CO Prod.	Surface Volume
D	1358	2.7		17.9
C	1348	3.3		8.8
H	845	1.9		11.5
O*	1386	1.1		6.0
F	769	2.5		7.5
B	697	1.1		7.8
	Avg. 1067	Avg. 2.1		Avg. 9.9
N*	1322		8.3	6.5
R*	820		3.4	8.6
P*	743		1.4	13.2
Q*	795		2.0	7.5
M	697		2.2	10.9
U*	429		1.6	10.4
T*	321		1.9	9.5
	Avg. 732		Avg. 3.0	Avg. 9.5

*Substrate for gas production added.

increase in pCO, thus necessitating continuous production of CO to prevent float collapse. For example, if the diffusion constant holds for higher pressures, then at 30 atmospheres the float must produce 30 times the quantity of gas it makes at one atmosphere to counter diffusive loss in the same length of time, if factors such as float volume, surface area, and wall thickness remain relatively constant. That is, the amount of gas lost by diffusion is directly proportional to the partial pressure gradient of that gas.

Carbon Available For Gas Production

If the above assumptions hold true, at a depth of 300 m in the sea, a nanomian with a float volume of 1 mm³ and an area of 10 mm² must produce 30 mm³ of CO to counter hydrostatic pressure plus about 4 mm³ per hour to compensate for diffusive loss. This quantity of gas equals 16 µg of carbon per day plus an additional 2 µg per hour. These figures indicate that a fairly large quantity of organic matter must be ingested in order to meet the rather large and continuous need for biochemical substrate for carbon monoxide production.

The gastrovascular fluids of *Physalia* are rich in peptides and amino acids including serine,^{29,30} the substrate of choice for gas production.¹⁷ In all likelihood similar analyses will be found for *Nanomia*. Little is known of the food habits of siphonophores, but logical sources of protein carbon are small crustaceans such as copepods or young euphausiids. In captivity *Nanomia* readily accept young brine shrimp (*Artemia*) and young copepods (*Tigriopus*).³¹ Conceivably, organic detritus which forms the often abundant particulate "snow" commonly seen throughout much of the water column during deep submersible dives could also be utilized.³² Swarms of adult euphausiid shrimp have also been seen at or near depths where nanomians occurred in numbers.* Availability of protein carbon for gas production is therefore probably not the

* Observations made during DEEPSTAR Dives 182 and 184³⁴ (observers, Pickwell and Adams) showed, in agreement with the observations of Barham,⁹ that particularly in near-shore waters, physonect siphonophores are numerous at depths of the DSL and euphausiid shrimp are often abundant at overlapping depths just above the siphonophores.

problem initial calculations might seem to indicate. For example, the copepod, *Calanus helgolandicus*, has a dry weight of organic substance of about 12 μg per copepod.³³ Assuming 20 percent is protein, each copepod then possesses about 2.4 μg of protein of which about 60 percent is carbon, or about 1.4 μg . A nanomian with the representative dimensions stated above would thus be required to capture little more than two to three copepods per hour to meet its gas secretion needs as well as most respiratory and nutritional demands.

Nonsecretory Oxygen Consumption

It is of further interest to determine a basal or nonsecretory level of oxygen consumption. As reported previously,¹⁸ the author performed a series of experiments showing low levels of O_2 consumption as probably representing nonsecretory rates. Since some degree of gas secretion was seen in nearly all of the specimens of table 2, it is probable that a number of those shown in the previous work secreted some small quantities of CO although insufficient data were available to prove this. Siphonophores or closely allied forms which do not secrete gas would therefore be of value in providing the desired nonsecretory levels of oxygen consumption.

An opportunity to perform such experiments arose in the summer of 1966 during the FASOR II cruise in the western Pacific (table 1) where a number of specimens of the Portuguese Man-of-War, *Physalia physalis* (L.) (fig. 7) were collected and experimented upon while at sea. Collections of the Sail-by-the-Wind, *Velella velella* (L.) (fig. 8) and its ally, *Porpita porpita* (L.) (fig. 9) were also taken and utilized in experiments.

While *Velella* and *Porpita* are not now regarded as true siphonophores,³⁵ they are considered closely enough related to provide a valid comparison to physonect siphonophores. Neither species possesses a gas gland. *Physalia* does have a well-developed gas gland, but the adult form lives entirely upon the surface of the sea and its gas secretion should be only sporadic or at a very low rate. This is supported by the observations of a number of workers that the percentage of CO in the float of *Physalia* generally is in the range of 5 to 15 percent and has never

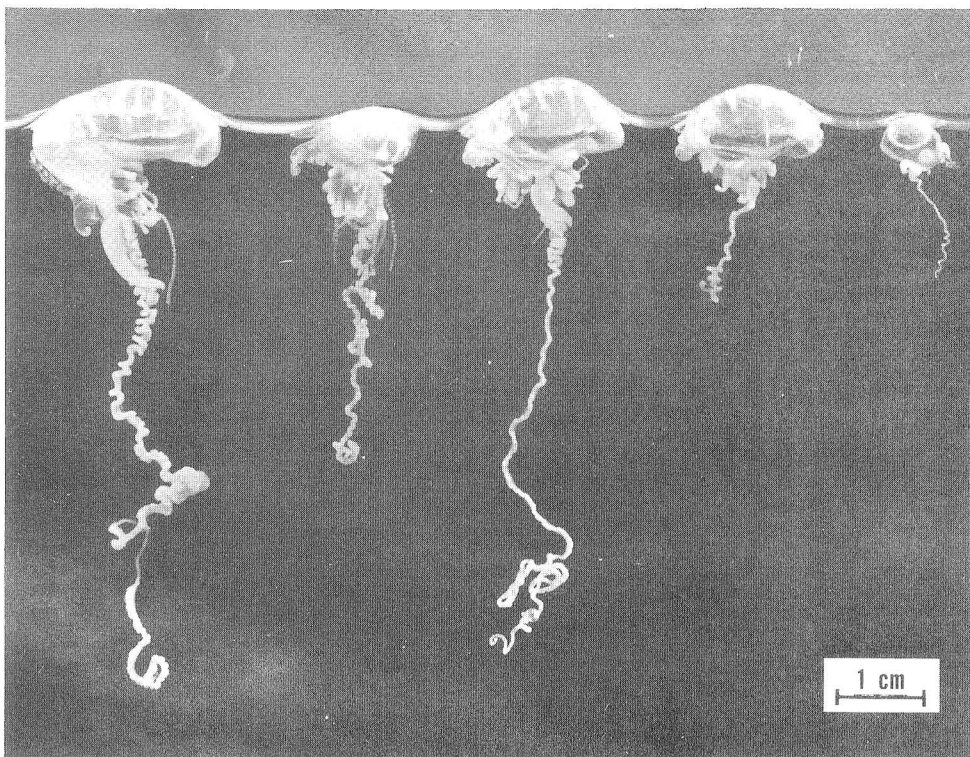


Figure 7. Preserved specimens of the Portuguese Man-of-War, *Physalia physalis* L.; collected approximately 70 miles east of Formosa. Specimens shown were used in microrespirometry experiments (table 8).

been demonstrated to exceed 25 or 30 percent^{17,27,28,36} (cf. Appendix E). No CO has ever been found in the float of *Velella* and in freshly caught specimens which were collected before stranding; the largest part of the float gas is nitrogen, supporting the early observation that any oxygen entering the float is probably consumed in the respiratory process³⁷ (Appendix E). This is further borne out by the relatively high percentages of CO₂ contained in the float.

The results of a series of respiratory experiments performed on these three surface-dwelling species utilizing the Scholander microrespirometer^{38,39} (Appendix B) are summarized in tables 8 and 9.

The average values representing *Velella* and *Porpita* and that of *Physalia*, are taken as representative of nonsecretory levels of oxygen consumption. For ease of comparison with data presented in this report and particularly with values given in the recent literature,^{27,28} the rates in tables 8 and 9 have again been adjusted to 20° C by the Van't Hoff method (referred to as VH₂₀).

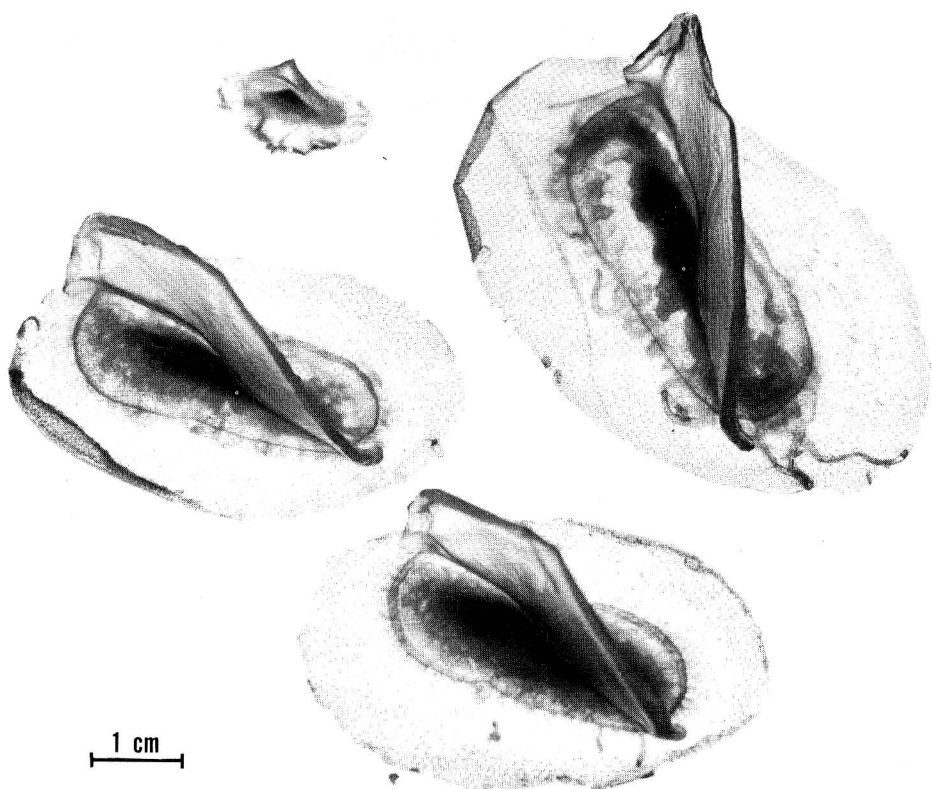
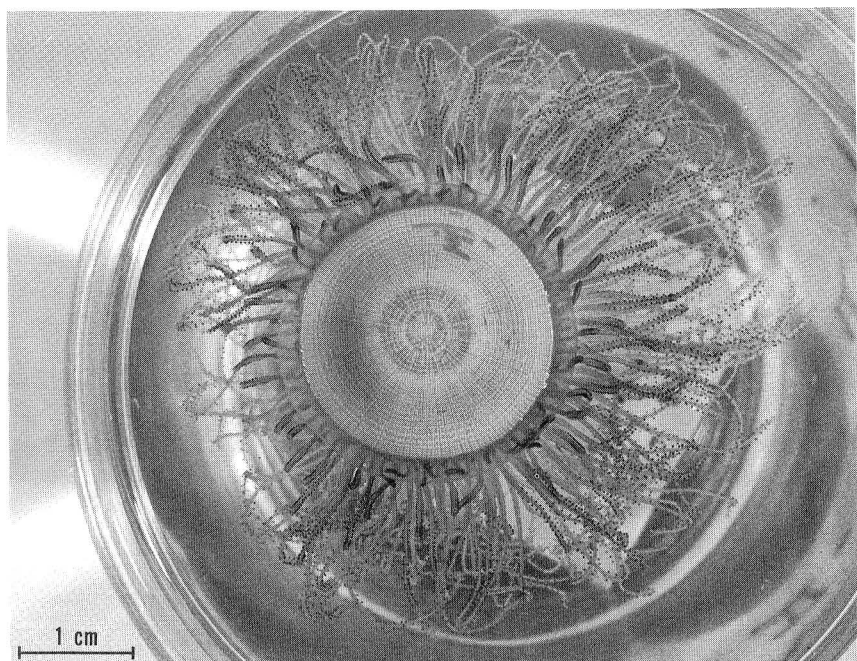


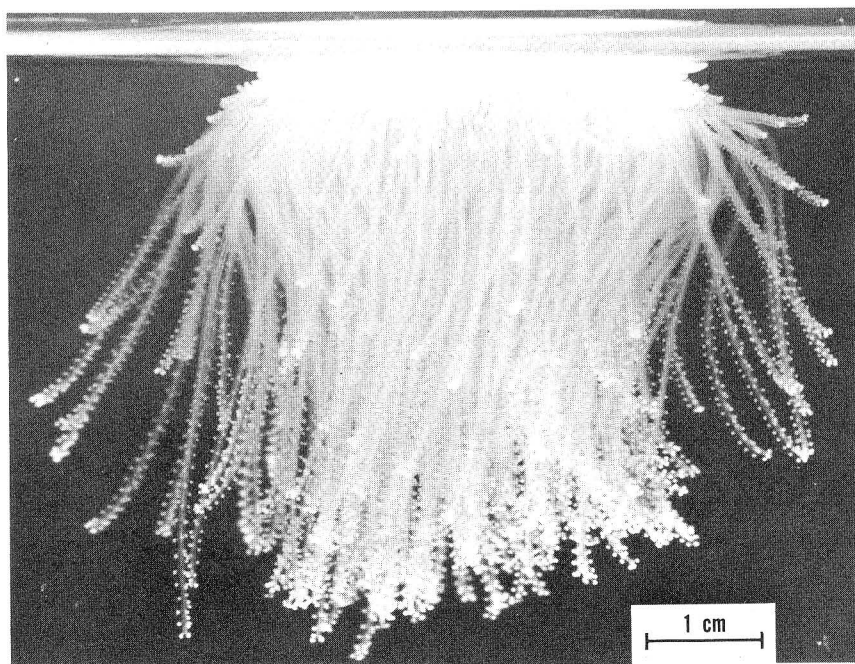
Figure 8. Preserved specimens of the Sail-by-the-Wind, *Velella velella* (L.) collected in the East China Sea. The larger specimens are similar to those used in microrespirometry experiments (table 9).

In general, after an initial period of stabilization, the rates of O_2 uptake are approximately linear showing only a very gradual decline, if at all (figs. 10, 11, 12). However, in longer experiments the reduction in oxygen consumption with time becomes more pronounced and care must be taken in defining the rate as being only an average for the time interval in question as is done for the syringe experiments (cf. Experiment 8, table 8 and Experiment 7, table 9).

Following the establishment of a reliable series of base-line values for nonsecretory O_2 consumption, it was desirable to run a series of experiments on *Nanomia* that would more clearly demonstrate the rates of O_2 uptake when neither pH, CO_2 nor CO might become important inhibitory factors. These experiments were run in the Scholander micrometer respirometer⁴⁰ employed to a limited extent in earlier work and discussed in detail in that report¹⁸ (see also Appendix B).



A



B

Figure 9. Preserved specimens of *Porpita porpita* (L.) collected in the South China Sea; A, plan view from above; B, lateral view. A and B are different specimens.

TABLE 8. RESPIRATION OF *Physalia physalis**

Experiment Number	Blotted Wet Wt. (mg)	Float Length (mm)	Sea Surf. Temp. at Time of Capture (°C)	Total Exper. Time (hr:min)	Water Bath Temp. (°C)	Avg. Respiratory Rate** (mm ³ /mg/hr)	Respiratory Rate STPD (mm ³ /mg/hr)	Resp. Rate Adjusted to VH ₂₀ † (mm ³ /mg/hr)
1	123.3	20	28.3	4:42	30.4	0.040	0.034	0.017
2	166.0	20	28.3	4:42	30.4	0.033	0.028	0.014
3	65.2	15	28.3	4:42	30.4	0.053	0.045	0.022
4	73.2	16	28.3	4:42	30.4	0.047	0.040	0.019
5	156.0	12	28.3	4:42	30.4	0.027	0.023	0.011
6	383.4	22	28.3	4:42	30.4	0.030	0.025	0.012
7	12.8	6	28.3	4:42	30.4	0.009	0.008	0.004
8a)	401.9	30	22.8	3:32	24.7	0.040	0.034	0.025
b)				4:10		0.023	0.020	0.014

*Performed with the Scholander microrespirometer (refs. 38, 39).

**Corrected for thermobarometer control.

†Rates calculated by Van't Hoff equation assuming a Q₁₀ of 2.

TABLE 9. RESPIRATION OF *Velella velella* AND *Porpita porpita* *

Experiment No.	Blotted Wet Weight (mg)	Float Length (mm)	Sail Length at Base <i>Velella</i> (mm)	Sea Surf. Temp. at Time of Capture (°C)	Total Exper. Time (hr:min)	Water Bath Temp. (°C)	Avg. Res- piratory Rate** (mm ³ /mg/hr)	Respiratory Rate STPD (mm ³ /mg/hr)	Resp. Rate Adjusted to VH ₂₀ † (mm ³ /mg/hr)
<i>Velella</i> 1	1273.4	35	30	23.3	3:08	27.0	0.040	0.034	0.021
2	1069.2	36	32	23.3	3:08	27.0	0.029	0.025	0.015
3	1183.9	36	29	23.3	3:08	27.0	0.036	0.031	0.019
4	1949.4	49	39	23.3	3:08	27.0	0.015	0.013	0.008
5	1830.5	50	39	23.3	3:08	27.0	0.019	0.016	0.010
6	1872.8	47	43	23.3	3:08	27.0	0.023	0.020	0.012
7a)	1753.5	44	38	22.8	3:32	24.7	0.023	0.020	0.014
b)					4:10		0.017	0.015	0.011
8	42.9	9.5	9.5	20.4	4:17	21.5	0.024	0.021	0.019
<i>Porpita</i> 9	2980.1	23 diam.		23.3	2:40	27.0	0.031	0.027	0.017

*Performed with the Scholander microrespirometer ^{38, 39} except No. 8, which was performed with a syringe.

**Corrected for thermobarometer control.

† Rates calculated by Van't Hoff equation assuming a Q₁₀ of 2.

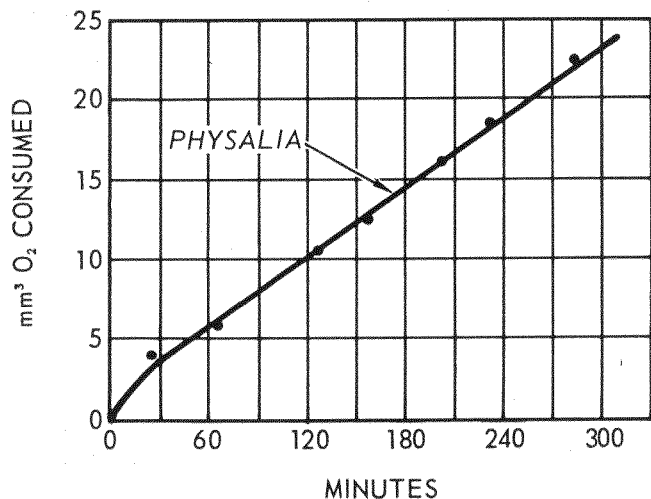


Figure 10. Oxygen consumption of *Physalia*. This plot is from Experiment No. 1, table 8. Temperature 30.4° C, uncorrected for standard conditions.

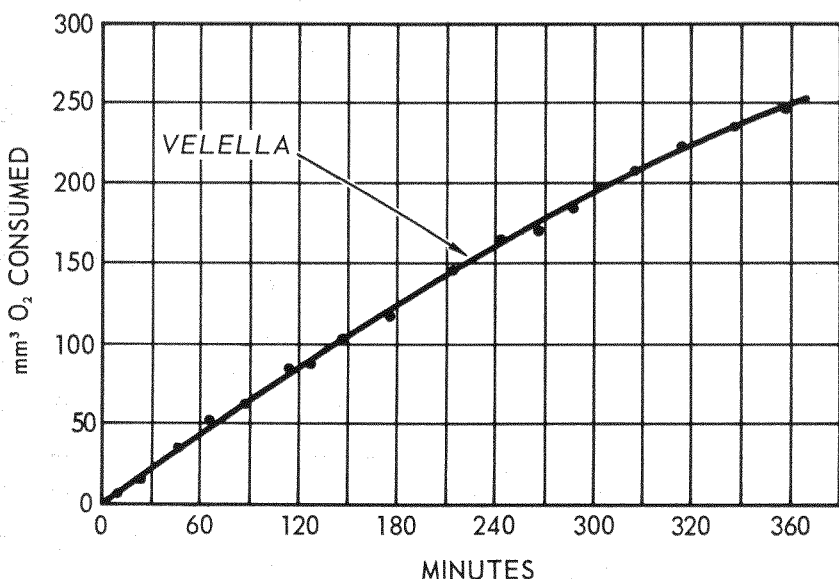


Figure 11. Oxygen consumption of *Velella*. This plot is from Experiment 7a and b, table 9. Temperature 24.7° C, uncorrected for standard conditions.

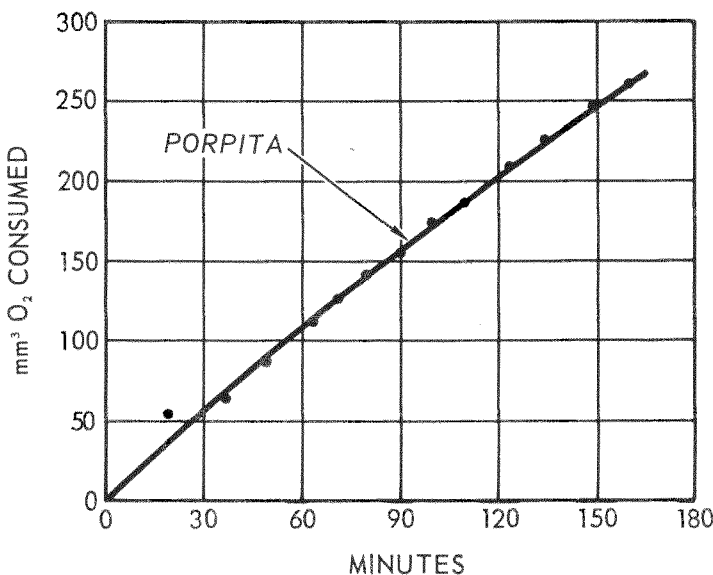


Figure 12. Oxygen consumption of *Porpita*. This plot is from table 9. Temperature 27.0° C, uncorrected for standard conditions.

Data from these runs are summarized in table 10. In the first group of experiments a single loop of wire suspended over the floating pneumatophore in the reaction vessel held a drop of concentrated KOH acting as CO₂ absorber. In the second group a double loop was employed (fig. 13), the second loop holding a drop of 0.02N palladium chloride as CO absorber^{41,42} (Appendix F).

The average for the two groups seems to indicate a 0.1 mm³ difference due to alleviation of the back pressure of CO that countered the change in gas phase volume due to oxygen uptake and coincident movement of an indicator drop (see fig. 5, reference 18 or fig. 3, reference 40). However, it seems probable that the CO absorber was not in great enough concentration to effectively remove all of the CO produced. Thus, in spite of the difference in group averages, the range of values for the two groups is, to a large extent, comparable and it seems probable that the maximum O₂ consumption that can be observed by this method may be still somewhat higher (note, however, Float 2, table 10).

Oxygen consumption determined by this method is generally approximately linear over a period of one to several hours with a variable period of stabilization at the start and a gradual leveling tendency (figs. 14, 15, 16). Therefore, the low values appearing

TABLE 10. RESPIRATION OF INDIVIDUAL FLOATS OF *Nanomia Bijuga*

Specimen No.	Blotted Wet Wt. (mg)	Total Experiment Time (hr:min)	Avg. O ₂ Consump. Corrected for Control (mm ³ /mg/hr ± 0.005)	O ₂ Consump. Corrected for STPD (mm ³ /mg/hr)	Van't Hoff 20°C (Assume Q ₁₀ = 2) (mm ³ /mg/hr)	Remarks
Group A: KOH only						
1	2.5	4:37	0.555	0.531	0.978	
2	3.4	4:35	0.488	0.467	0.860	Bubbles in g.g. and produced at end, thus proving CO production during run.
3	6.7	4:36	0.168	0.161	0.296	
4	5.6	4:07	0.088	0.084	0.155	
5	3.3	3:46	0.230	0.220	0.405	
6	5.0	2:04	0.157	0.150	0.276	
7	5.0	2:01	0.092	0.088	0.162	
					Avg. 0.447	
Group B: KOH and PdCl ₂						
8	3.5	6:34	0.519	0.496	0.915	
9	2.5	3:52	0.454	0.434	0.798	
10	4.2	3:38	0.172	0.165	0.304	
11	2.6	3:17	0.149	0.143	0.263	
12	5.8	2:49	0.247	0.236	0.435	
					Avg. 0.543	

*All at 11.2 ± 0.3°C. All in good condition at end of run. Experiments performed with Scholander micrometer respirometer (see refs. 18 and 40).

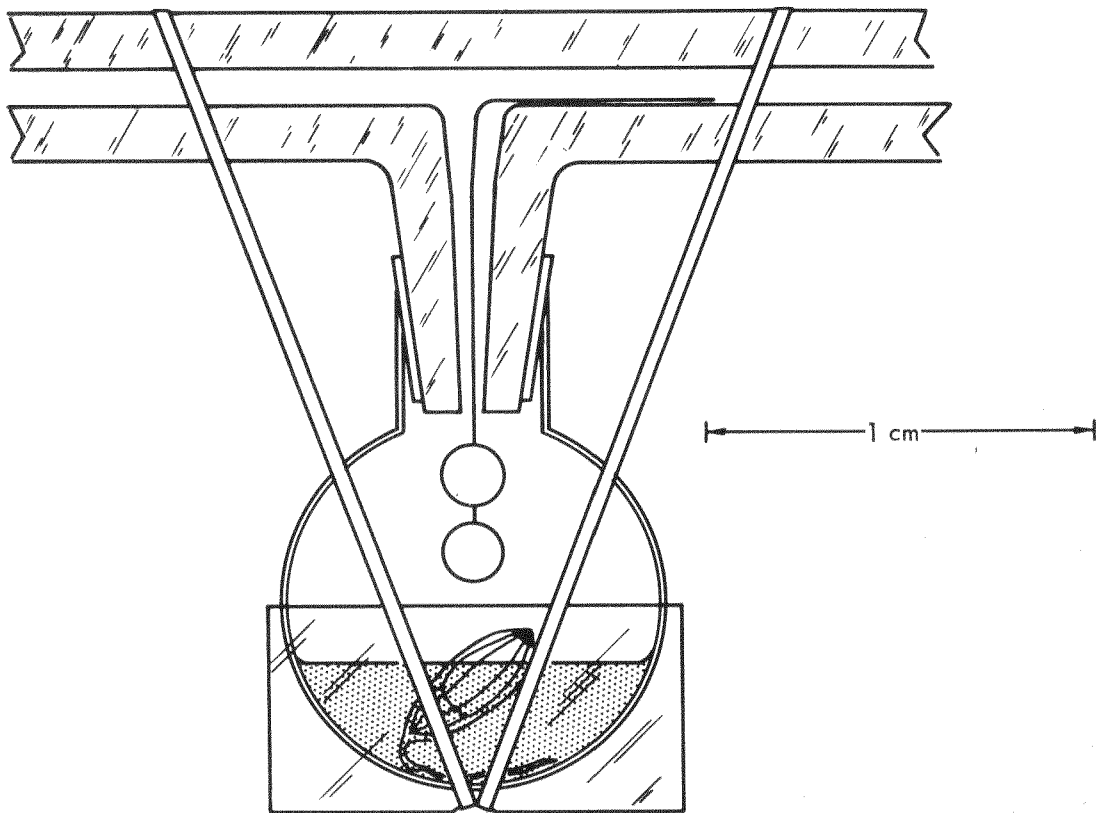


Figure 13. Respiratory chamber for micrometer respirometer showing double wire loop for holding drops of absorber. Upper loop holds KOH, lower loop holds PdCl_2 . Nanomian pneumatophore floats in seawater below loops. The chamber is seated in a short length of Tygon tubing and the entire assembly is held in place on the capillary "T" with rubber bands.

in Group A, table 10, probably are not the result of an inhibition, due to build-up of CO (cf. fig. 16 and results from Experiments O, Q, and others of table 2 and subsequent tables). The gradual decline in oxygen uptake is not considered a result of falling O_2 tension since the greatest quantity consumed, about 12 mm^3 (fig. 15), will reduce the oxygen in the 0.5 cc gas phase of the reaction chamber to no less than 18.5 percent. This is double the reduction resulting from the next highest rate (fig. 14) and probably does not approach a critical minimum.²³ Thus it seems, on the basis of these experiments, that additional efforts must be made employing stronger CO absorbers before maximum oxygen consumption values can be ascertained.

Oxygen consumption by *Nanomia bijuga* pneumatophores with attached fragments of stolon at 20° C ranged from 0.006 to

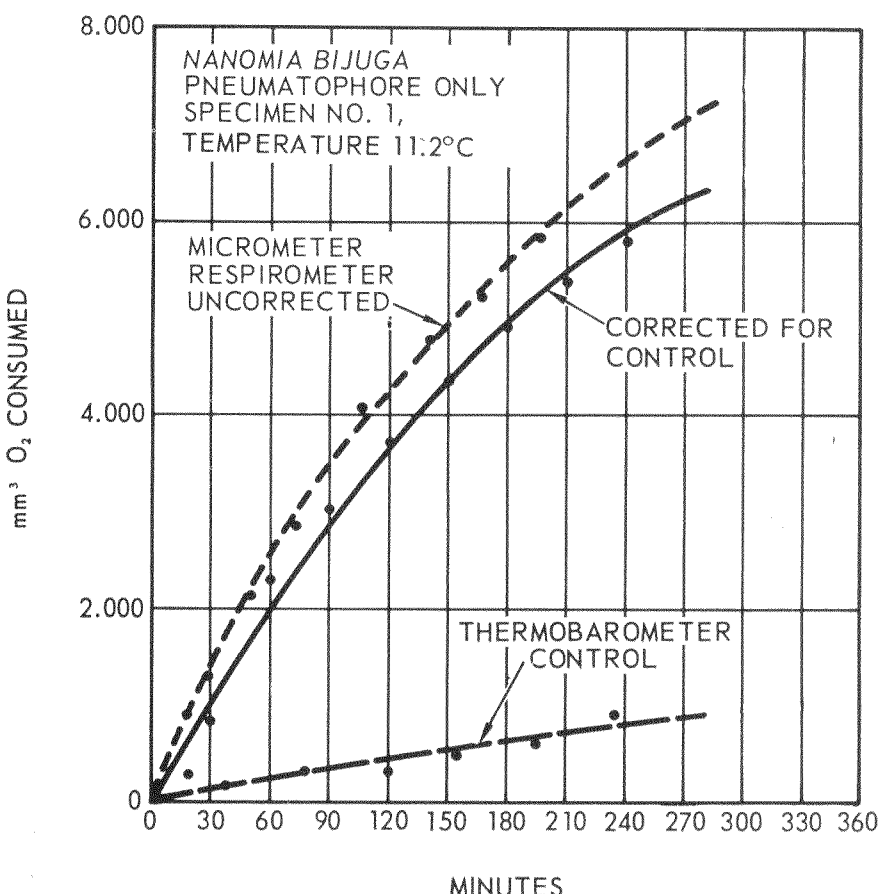


Figure 14. Oxygen consumption of *Nanomia*. Specimen No. 1, table 10, CO_2 only absorbed.

$0.430 \mu\text{l}/\text{mg}$ blotted wet weight/hr when determined by syringe respirometry (table 2). O_2 consumption determined by micrometer respirometer ranged from 0.162 to $0.978 \mu\text{l}/\text{mg}$ wet wt/hr at 20°C (table 10). O_2 consumption values for intact *Physalia* at 20°C lay in the range 0.004 to $0.025 \mu\text{l}/\text{mg}$ wet wt/hr (table 8), while values for *Velella* ranged from 0.008 to $0.021 \mu\text{l}/\text{mg}$ wet wt/hr at 20°C and a single value for *Porpita* was $0.017 \mu\text{l}/\text{mg}$ wet wt/hr (table 9). By comparison, Larimer and Ashby²⁷ found minced float tissues from *Physalia* pneumatophores to consume O_2 at 25°C within the range 0.075 to $0.170 \mu\text{l}/\text{mg}/\text{hr}$ when 0.001 M sodium succinate was added as a metabolic substrate.

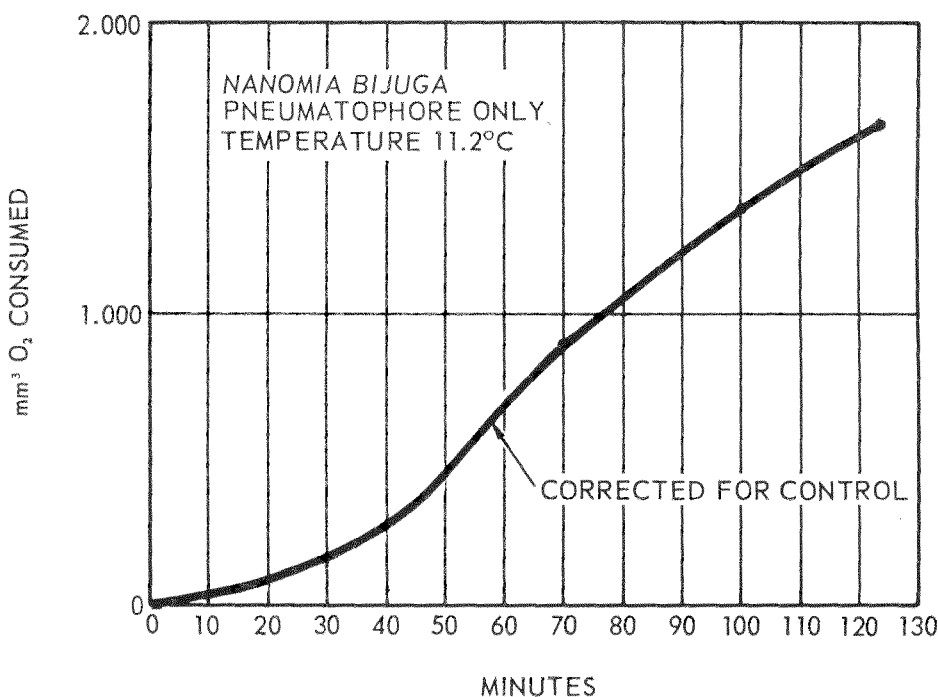


Figure 15. Oxygen consumption of *Nanomia*. Specimen No. 6, table 10, CO₂ and CO absorbed.

Carbon monoxide production by *Nanomia bijuga* determined by the syringe method, when substrate for gas production (L-serine) was added, ranged from 0.623 to 4.500 $\mu\text{l}/\text{mg}$ 10% gas gland/hr at 20° C for pneumatophores remaining alive at the end of the run. Lacking added substrate for gas production, CO secretion ranged from 0.746 to 2.060 $\mu\text{l}/\text{mg}$ 10% g.g./hr (table 2). When producing bubbles the nanomian gas gland can increase these figures by at least 200 times (see table 11 and discussion in the following section). By comparison, Hahn and Copeland²⁸ reported that portions of the excised gas gland of *Physalia*, when incubated with added substrate for gas production at 22° C, produced CO at rates from 0.280 to 1.075 $\mu\text{l}/\text{mg}/\text{hr}$.

These data suggest that the nanomian gas gland is a more active producer of CO than the gas gland of *Physalia*. This observation is not surprising in view of the daily requirement for production of several times its float volume of CO which must be met by *Nanomia* as a result of its known vertical migrations.

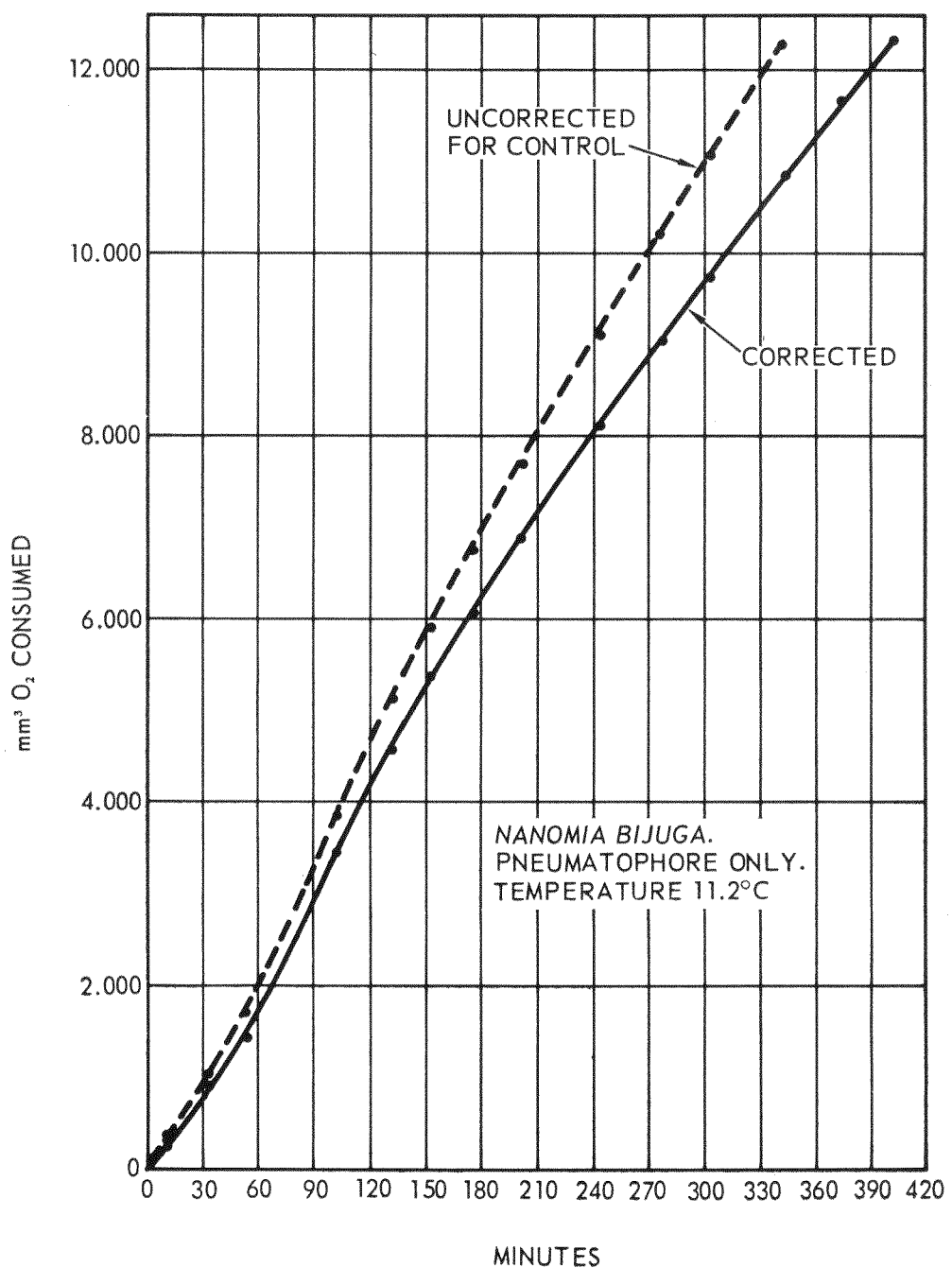


Figure 16. Oxygen consumption of *Nanomia*. Specimen No. 8, table 10, CO₂ only absorbed.

TABLE 11. VOLUNTARY BUBBLES PRODUCED BY NANOMIAN
PNEUMATOPHORES* (Continued on page 46).

	Pneumatophore	Gas Phase Dimens. (mm) (length X width)	Gas Phase Volume (mm ³)	No. of Bubbles Produced When Produced (before, after placing in water bath)	Time Req'd. to Produce Bubbles	Temp (°C)	Volume of Bubbles (mm ³)	Gas Composition of Bubbles (%)	Estimated Rate of Gas Prod. Based on Bubble Prod. (mm ³ /mg 10% g.g./hr)	Estimated Rate STPD/VH ₂₀ (mm ³ /10% g.g. hr)	Remarks
D	2.25 X .50 after expulsion	0.29	1	Before	10-30 sec	24.5	0.13				
C	a)3.25 X .87 before expulsion b)3.12 X .75 after expulsion	1.30	1	Before	10-30 sec	24.0	0.51				May be case 2; cf. Float B.
N*	a)3.12 X 1.12 before expulsion b)3.12 X 1.37 after expulsion	2.07 3.09	3	1)Before 2)In syringe before water- bath 3)In syringe before water- bath	10 min	21.8 3)0.37	1)0.76 2)0.17 3)0.37	CO 87.4 196 (349 including increase in float vol.)	176 314	155 277	No detectable CO ₂ or O ₂ . Only instance of bubbles with added substrate.
A	2.25 X .50	0.29	1	Before	10-30 sec	21.5	0.13	CO 66.6			No detectable CO ₂ or O ₂
H	4.00 X .87	1.60	4	Before	5 min	22.2	1)0.06 2)0.13 3)0.22 4)0.06		20.1	18.0 15.5	

TABLE 11. (Continued).

Pneumotophore Gas (length Gas No.)	Phase X width (mm)	Dimens. (mm)	Volume (mm ³) Produced before bath	Rate of Gas Prod. STPD/(NH ₃) g./min.				
				No. of Bubbles Produced in water when placing gas phase No. in water bath	Temp (°C) Read. to Bubble Volume (mm ³)	Estimated Rate of Bubble Composition (%) Based on Gas Bubbles (mm ³) Estimated Rate of Gas Production (mm ³ /min.)	Remarks	
F	a)4.38 X 1.13	2.90	8	1)Before 2)Before 3)Before 4)After, in syringe 5)After, in syringe 6)After, in syringe 7)After, in syringe 8)After, in syringe	10 min for Nos. 1-3 inc 5 min for Nos. 4-8 inc	22.2 22.9 3)1.40 4)0.17 5)0.37 6)0.78 7)0.11 8)2.51	1)0.13 2)0.13 3)CO 76.3 4)CO 76.3 5)does not include increase in float vol. 141 158	29.7 25.5 141 115
	b)4.24 X 2.37	12.55					No detectable CO ₂ or O ₂ . In float at end: 82.2% CO, 4.4% O ₂ no CO ₂ .	
	c)3.87 X 1.87	7.13						
M	a)3.25 X .75 before expulsion	0.95	1	In syringe before water bath	10-30 sec 21.6	0.51 CO 55.9	No detectable CO ₂ or O ₂ . Many bubbles in gas gland at time of expulsion of bubble.	
	b)2.87 X .87 after expulsion	1.15						
B	a)4.12 X 1.00 before expulsion	2.16	1	Before	10-30 sec 21.0	0.68		
	b)3.62 X .75 after expulsion	1.60						

*Substrate for gas production added.

BUBBLE PRODUCTION

It will be shown below that the most rapid rates of carbon monoxide production were associated with discharge of bubbles from the pneumatophore. A second type of bubble expulsion has often been observed which is not associated with gas production. In the latter case the float continues to periodically expel gas until it is nearly emptied and has become shrunken and shriveled in appearance. Both sets of conditions have been observed and are recorded in the earlier literature.^{25,26} However, the second type of expulsion is poorly understood. No gross movements of the body wall or apical sphincter are evident, even under magnification, in conjunction with bubble expulsion of either type. No muscle flexure or peristaltic motion has yet been consistently observed.

In Case 1, where bubble production is associated with gas secretion, it is probable that upon surpassing some critical internal pressure, a bubble simply bursts forth and breaks off from the tip of the float when the buoyant force on the bubble becomes great enough. This can be termed "passive production" in opposition to the "active production" of Case 2 where a float not producing gas contrives to rid itself of all or most of its gas phase even when the gas is under no pressure greater than ambient. The two situations are defined as follows: Case 1: bubble expulsion with gas secretion; the float volume following expulsion may be less than, equal to, or greater than the starting volume. Case 2: bubble expulsion without gas secretion; the final float volume is always less than the starting volume; the sum of the final float volume and total volume of expelled bubbles is never greater than the starting float volume (for example, possibly floats C and B, table 11 and Float 11, table 12).

Figures 17 and 18 present a series of close-up photos, taken aboard ship, of freshly captured nanomian pneumatophores in the act of producing bubbles. These represent Case 1 where bubble expulsion does not appreciably reduce the volume of the float gas phase nor leave the float in a shriveled condition. In figure 18, as further evidence of gas secretion, note the presence of bubbles within some of the floats in the basal gas-gland region.

Although no clear-cut movement or flexion is evidenced by the pneumatophore (such movements are reported in earlier literature, however; see ref. 25), the addition of MgSO₄ to the

TABLE 12. COMPARATIVE SIZES OF VOLUNTARILY EXPELLED BUBBLES*

Float	Blotted Wet Weight (mg)	Beginning Volume of Float Gas Phase (mm ³)	Bubble Radius (mm)	Bubble Volume (mm ³)	Bubble Radius (mm)	Bubble Volume (mm ³)	Bubble Radius (mm)	Bubble Volume (mm ³)	Bubble Radius (mm)	Bubble Volume (mm ³)	Ending Volume of Float Gas Phase (mm ³)	Remarks
1	2.0		0.55	0.70	0.49	0.37					1.34	Two bubbles in 10-12 minutes.
2	1.5		0.33	0.15	0.22	0.04					0.81	
3	3.0		0.24	0.06	0.31	0.13	0.56	0.74			0.63	
4	0.8		0.22	0.04							0.65	
5	3.1		0.25	0.06	0.18	0.03	0.25	0.06	0.31	0.13	0.69	4 bubbles in 2 minutes.
6	5.4		0.38	0.22	0.44	0.35					0.61	
7			0.62	0.99								Volume det. by calibrated capillary.
8		4.65	0.45	0.38	0.65	1.13	0.75	1.72			3.14	Bubbles in gas gland during bubble expulsion.
9	6.6	4.92	0.35	0.17	0.42	0.29					7.11	Addn'l 5 bubbles expelled. Total = 7.
10	3.0	0.25	0.24	0.06	0.20	0.03	0.25	0.06			-	Addn'l 6 bubbles expelled. Total = 9.
11		0.75	0.35	0.17	0.25	0.06	0.40	0.27				Beginning vol. det. made after 1st bubble. Float shriveled following expulsion.
12		0.26	0.40	0.27							0.14	

*Temperature, 24 to 26°C. No substrate for gas production.

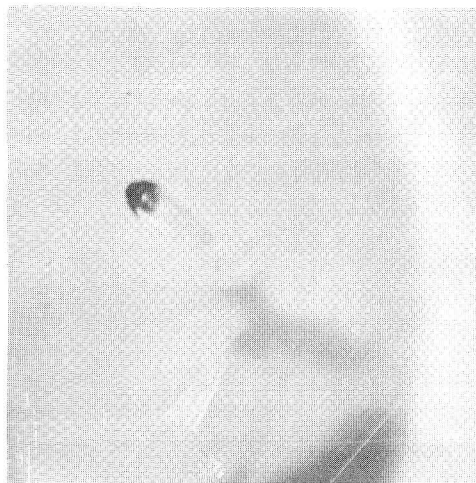
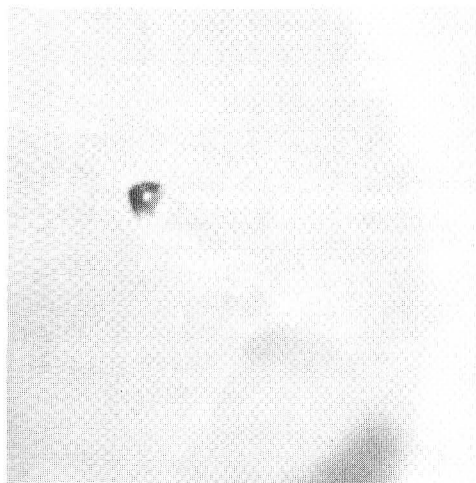
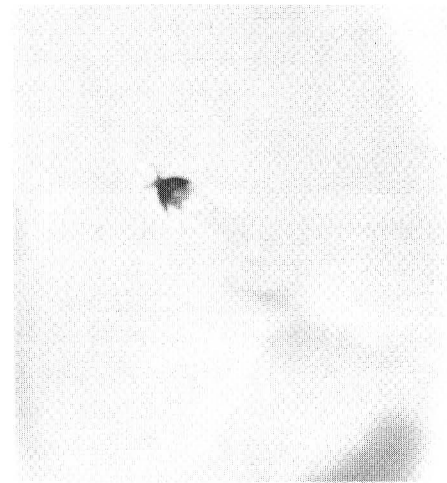
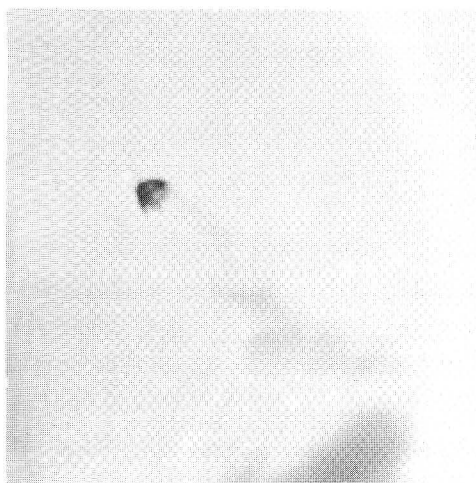
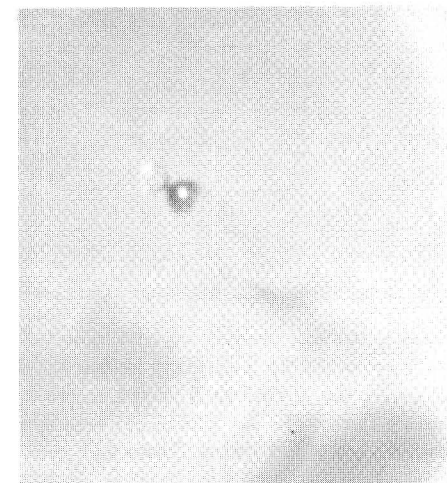
**A****D****B****E****C****F**

Figure 17. Successive stages in the production of a single bubble by a nanomian pneumatophore. In A, the bubble is barely visible at the pigmented tip where it begins to extrude through the apical pore. (Approximately $\times 5$).

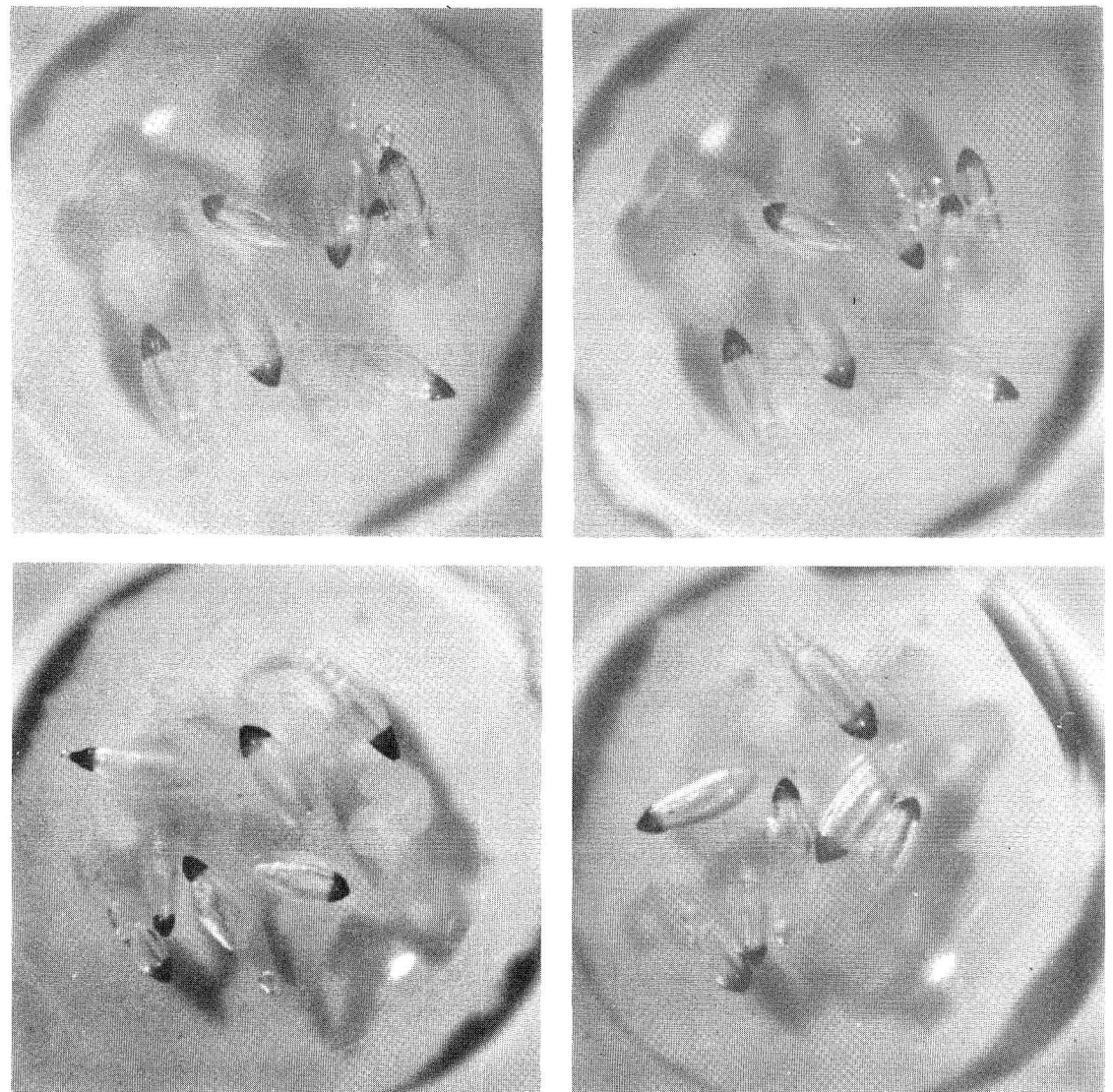


Figure 18. Bubble production (A). The bubble after expulsion floated to the left (B), where it remained for some time before bursting. If expelled at depth with the same dimensions, the bubble in B would be resonant at 12 kc/s at 100 m and 24 kc/s at 400 m, according to theory. An additional bubble is produced in C, and in D are shown grape-like clusters of bubbles forming in the gas gland region of two floats. (Approximately $\times 3$).

seawater around the float serves to "freeze" or immobilize the float when in the act of expelling a bubble. This is seen in the photos shown in figure 19 which were taken aboard ship through a compound microscope, again using fresh-caught material. The fact that magnesium sulfate produces this effect suggests that there may actually be some muscular function associated with the expulsion of bubbles.

Data on the bubbles produced by specimens listed in table 2 are given in table 11. Here it can be seen that upon occasion, bubbles were produced in rapid sequence, were generally high in carbon monoxide, and in the majority of cases arose in experiments where no substrate was added. Estimates of rate of gas production which are given in table 2 do not include these rapid bubble rates unless bubble expulsion occurred inside the syringe and the bubbles were not removed before incubation.

In table 12, as well as in table 11, are presented the volume ranges and radii for sequential bubbles arising from individual floats. It is immediately apparent that no single float produces bubbles of uniform dimensions. Figure 20 presents these results graphically while figure 21 gives the total number of bubbles observed within arbitrarily chosen size limits. The majority of the floats in table 12 represent the Case-1 condition, but had they been allowed to remain in the dish at the table-top temperature of about 24° C, more than Float 11 might have shown Case-2 expulsion (cf. also Floats C and B, table 11). From these examples it seems the means of bubble expulsion, whether active or passive, has little effect on the size of bubbles produced relative to float volumes.

When the rates of bubble production by Case-1 pneumatophores are treated as representative of gas secretion rates as in table 11, and are then equated on a basis of weight of gas gland, they far surpass the already substantial rates given for the same pneumatophores in table 2. Bubbles produced were not used in calculating gas secretion rates for table 2 unless the bubbles were found in the syringe after incubation. Thus, at the stated temperatures, floats N, H, and F produced bubbles of gas in quantity sufficient to fill the starting volume of the float in slightly more than 13, 19, and 17 minutes, respectively. In addition, Float 5, table 12, produced bubbles at a speed to equal its starting float volume in about 9.5 minutes. The oxygen consumption during

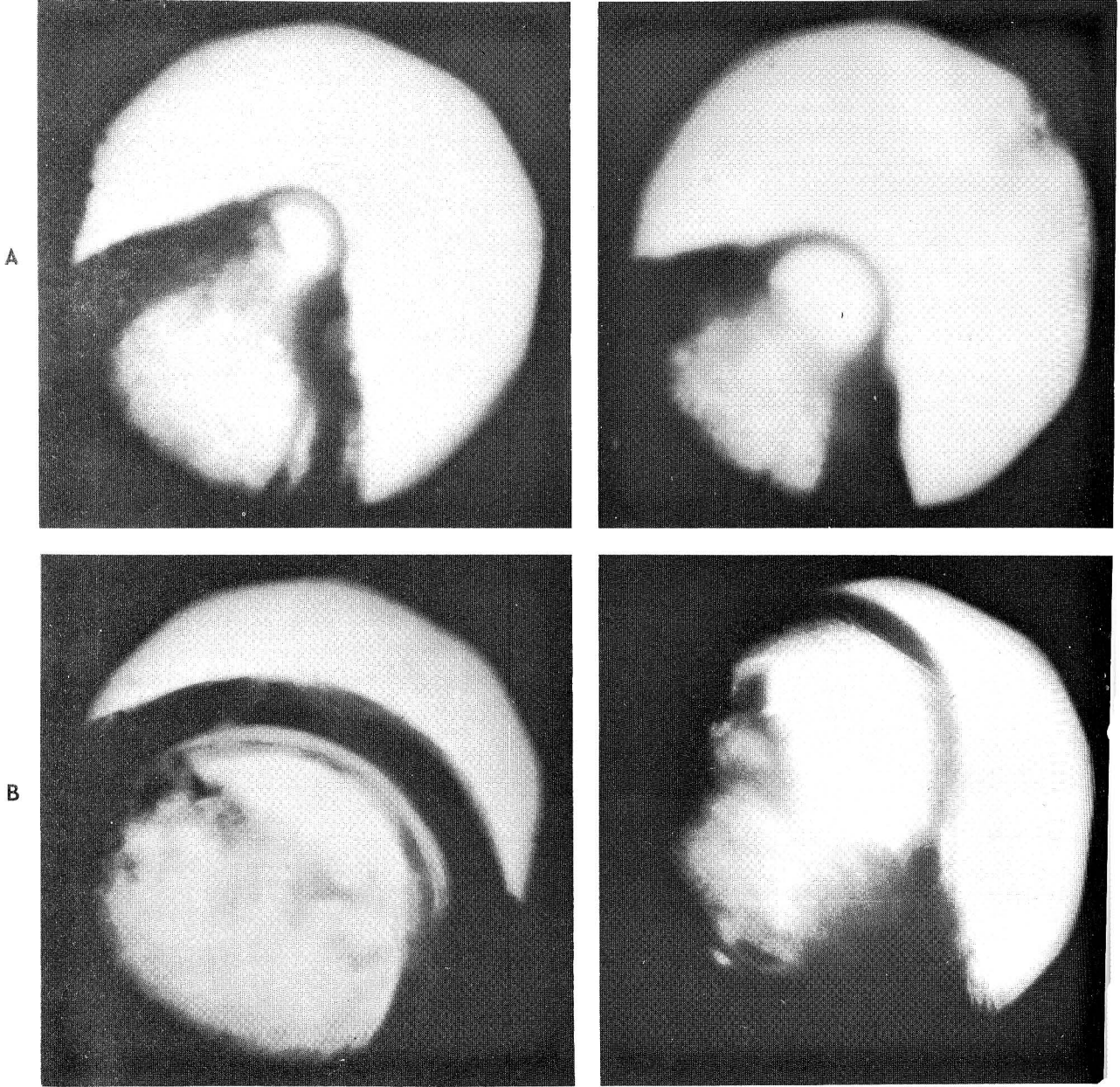


Figure 19. The pneumatophore tip with bubble "frozen" in act of being expelled by application of magnesium sulfate. A, B and D, successive stages of the same bubble which moved no further than shown in D. C shows a bubble stopped somewhat sooner than that in D by the same method. (Approximately $\times 60$).

● DENOTES DUPLICATE VALUES

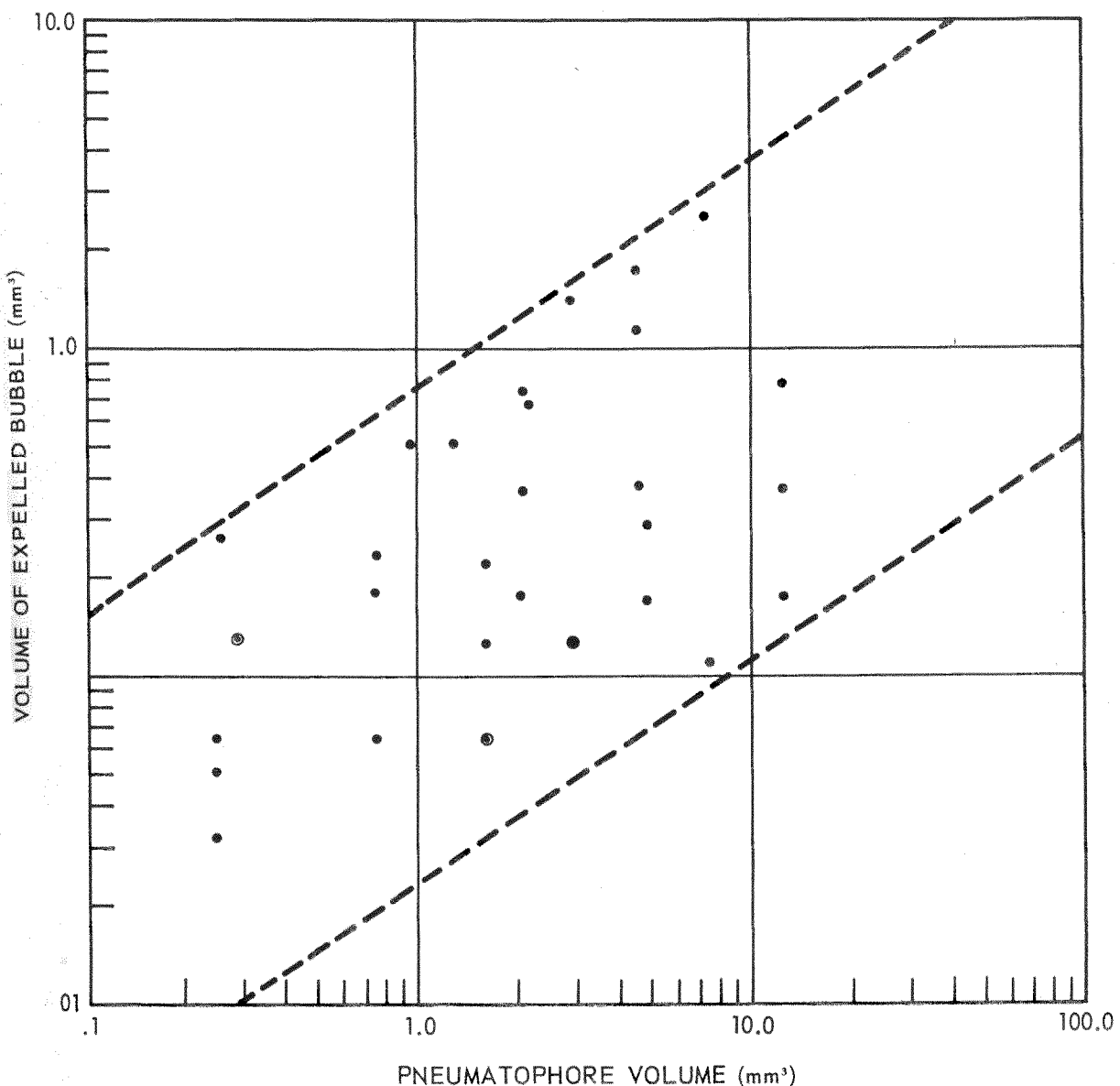


Figure 20. Pneumatophore volume vs. volume of individual extruded bubbles. Points vertically in line represent bubbles from the same pneumatophore. Dashed lines arbitrarily placed to encompass all observations.

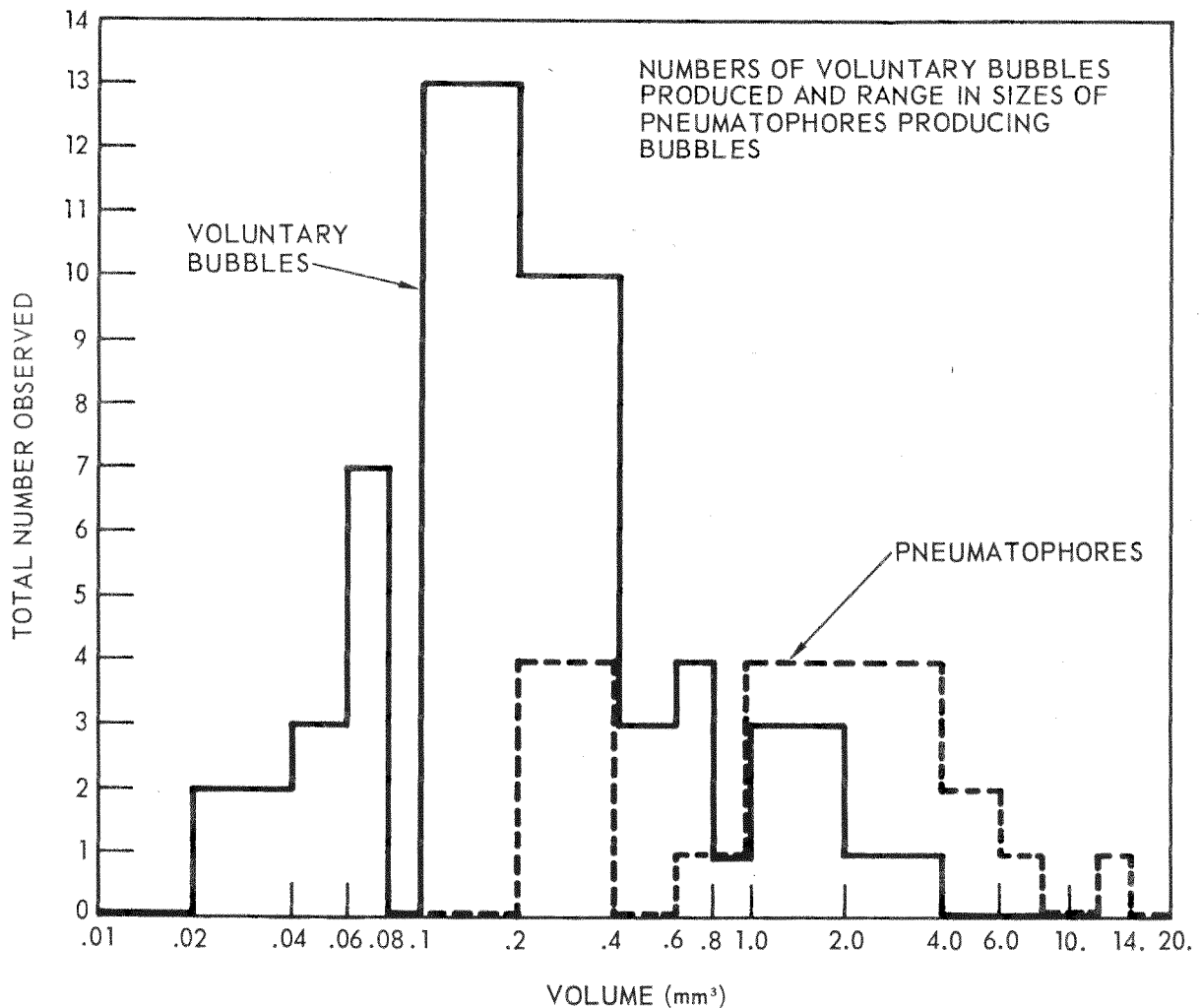


Figure 21. Total number of voluntary bubbles produced vs. bubble volume, and total number of bubble producing pneumatophores vs. pneumatophore volume. Solid line denotes bubbles, dashed line, pneumatophores.

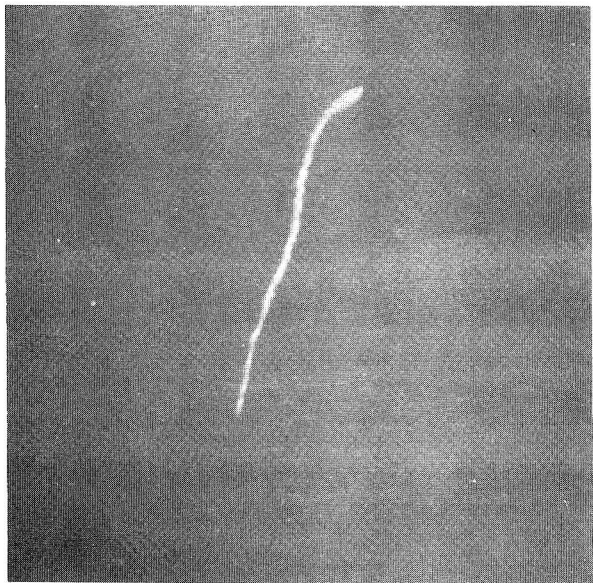
these brief periods of very rapid gas production is not known, but on the basis of material presented above it is assumed the O_2 uptake was elevated, perhaps to levels exceeding those in figure 4.

ACOUSTIC ASPECTS

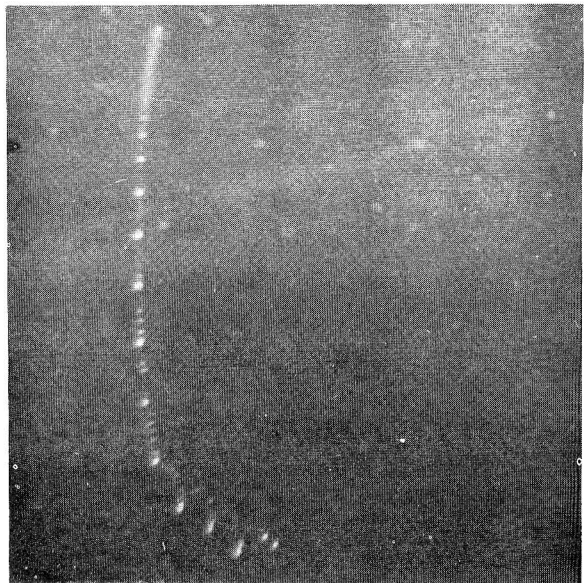
It now seems apparent that when physonectid siphonophores are present in concentrations sufficient to cause scattering layers, their contribution to the reverberation may be twofold; that is, a basic scattering effect due to the inflated pneumatophore, and secondary scattering from released bubbles. Bubbles must be vented during upward migration in the late afternoon, but may be released at other times as well. Thus, the response of *Nanomia bijuga*, when disturbed while floating at the sea surface, was to release a bubble from the float, thus altering the center of gravity of the colony and permitting it to quickly tip over and swim downward and away.^{25,26} Again, in the laboratory, intact specimens in tall glass cylinders periodically were observed to extrude gas, sink to the bottom, secrete additional gas, and after periods of 30 to 90 minutes reascend to the surface where the cycle was repeated²⁵ (see also Pickwell, *et al.*¹⁶). It seems reasonable, if this is common behavior, that this type of activity may be carried on to some degree at depth.

Dimensions of the gas phase of a number of nanomian pneumatophores have been presented in tables 2, 11, and 12. Previously,¹⁸ the volume range of the floats was stated to fall within 0.5 to 2.5 mm³.

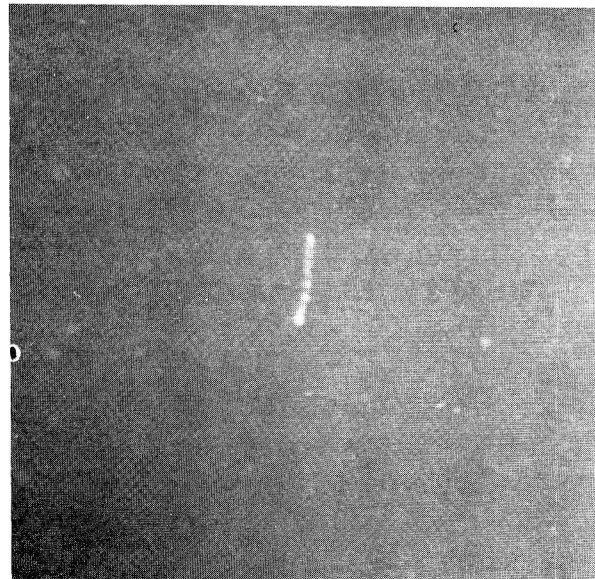
In the present report a few values exceed these limits in both directions. Thus, the observed range has been increased to 0.25 mm³ to 4.92 mm³ with an extreme to 12.56 mm³ (tables 11 and 12). The corresponding cross-sectional radii or minor semi-axes for these floats were 0.25 mm, 0.75 mm and 1.18 mm, respectively. Occasionally, floats of less volume may have even greater minor semiaxes with proportionately shorter major axes (see ref. 18 for a tabulation of the variation in float dimensions from two series of pneumatophores). Since the inflated pneumatophore is always buoyed in a vertical position relative to the sea surface regardless of the direction in which the colony may be moving (fig. 22), the minor semiaxis was employed in calculations of resonant frequency given in table 13. This orientation has been repeatedly observed by the author and others during dives in the DEEPSTAR 4000 (Dives 159, 170, 182, 183, and 184; also, E.G. Barham and I.E. Davies, personal communication). Directional sound propagation studies have yet to be performed upon these siphonophore floats in a manner similar to that which has been used on fishes (for example, see reference 43).



A



C



B



D

Figure 22. Photographs of nanomian siphonophores taken from DEEPSTAR. A, upward swimming nanomian, the pneumatophore clearly reflecting light; length of this specimen is estimated to be about 40 cm. B, a nanomian with stolon fully contracted; note, again, the glistening pneumatophore; estimated length, 15 cm. C, a relaxed, fully extended specimen in the feeding position; estimated length 60 cm. D, a downward swimming physonect; note that the shining float is buoyed upwards by its contained gas. A, from Dive 184; B through D, from Dive 170 (see table 1 for locations).

**TABLE 13. RESONANT FREQUENCIES OF VOLUNTARILY EXPELLED
BUBBLES AND OF BUBBLE-PRODUCING PNEUMATOPHORES**

Depth (m)	1 <i>R</i> (cm) Float 5, Table 12 Vol. = 0.03 mm ³	Minimum			2 <i>R</i> (cm) Float 12, Table 12 Vol. = 0.27 mm ³	Arbitrary Central			3 <i>R</i> (cm) Float 8, Table 11 Vol. = 2.51 mm ³	Maximum			
		<i>f_{ri(1)}</i> * (kc/s)	<i>f_{ri(2)}</i> * (kc/s)	<i>f_{rs}</i> * (kc/s)		<i>f_{ri(1)}</i> (kc/s)	<i>f_{ri(2)}</i> (kc/s)	<i>f_{rs}</i> (kc/s)		<i>f_{ri(1)}</i> (kc/s)	<i>f_{ri(2)}</i> (kc/s)	<i>f_{rs}</i> (kc/s)	
100	0.018	58	→	→	0.040	26	→	→	0.084	12	→	→	
200	0.018	80	→	→	0.040	36	→	→	0.084	17	→	→	
300	0.018	98	→	→	0.040	44	→	→	0.084	21	→	→	
400	0.018	111	→	→	0.040	51	→	→	0.084	24	→	→	
Voluntary Bubbles	4 Float 10, Table 12 Vol. = 0.25 mm ³	<i>R</i> = 0.039 Vol. as Sphere	<i>R</i> = 0.039 Vol. as Sphere	5 Float N, Table 12 Vol. = 2.07 mm ³	<i>R</i> = 0.079 Vol. as Sphere	<i>R</i> = 0.079 Vol. as Sphere	6 Float F, Table 11 Vol. = 12.55 mm ³	<i>R</i> = 0.145 Vol. as Sphere	<i>R</i> = 0.145 Vol. as Sphere	R = 0.145 Vol. as Sphere	R = 0.145 Vol. as Sphere		
	100	0.025 (minor semiaxis)	42	27	27	0.056 (minor semiaxis)	19	13	13	0.118 (minor semiaxis)	9	7	7
	200	0.025	58	37	36	0.056	26	18	18	0.118	12	10	10
	300	0.025	71	45	43	0.056	31	22	21	0.118	15	12	12
	400	0.025	81	52	50	0.056	36	26	24	0.118	17	14	13
	Pneumatophores												

**f_{ri}* = resonant frequency of an ideal bubble.

$$\frac{(d+10)^{1/2}}{R}$$
 In boxes 4, 5, and 6 the minor semiaxis of the pneumatophore taken as a regular prolate spheroid is treated as the radius of an ideal bubble. In the final two columns of these boxes the total volume of the pneumatophore is treated as a sphere to give *R*.

f_{rs} = resonant frequency of a real bubble, specifically a fish swim bladder in which the shear modulus, μ_0 , is included—(significant also for a siphonophore float?).

$$= 1.5 \sqrt{\frac{H+30}{3\sqrt{V}}}$$
 Note that the values of the final two columns in boxes 4, 5, and 6 appear to diverge with increasing depth. This is an artifact resulting from the generalizations used in deriving the short-cut formulas. Since μ_0 is a constant, the values will actually diverge slightly with decreasing depth from about 500 m. Below this depth both formulae from which the short forms were derived can be expected to give approximately the same result.

It was previously suggested¹⁸ that the floats may be poor reflectors or scatterers during the morning vertical descent and for some time thereafter due to possible partial deflation of the floats by increasing hydrostatic pressure and prolonged refilling times. However, it was shown above that refilling times, at least at 1 atmosphere, can be a matter of only a few minutes. In addition, observations during morning dives in DEEPSTAR revealed physonect floats to be fully inflated and effective light reflectors as shown in figure 22 and reported previously by Barham.⁹

Two important problems remaining to be solved in connection with the DSL are the relative contribution to scattering from specific types of organisms existing in a mixed population and the minimum number of a given size scatterer required to provide measurable volume reverberation.

The effective target area, or scattering cross section, σ_s , of an ideal resonant bubble at 1 atmosphere relative to its actual physical cross section increases by something in excess of three orders of magnitude when its ratio of circumference to incident wavelength is close to a peak value of 0.012.^{1,44} (See ref. 1 and ref. 44, p. 452, 460-467.) This falls off very sharply in either direction, such that at circumference-to-wavelength ratios of 0.01 and about 0.04 on either side of the peak, the ratio of σ_s to πr^2 is approximately 1000 times less. The resonant peak will shift to the right toward values greater than 0.01 as depth increases, however (see table 13). Thus, for any population of potential scatterers such as physonect siphonophores, displaying the range in dimensions seen in tables 2, 11, and 12, only a certain fraction of the total will behave as effective resonant scatterers in the presence of narrowband sound even when the frequency is expected to favor resonance. On the other hand, presumably only about one-thousandth as many scatterers are required, if resonant, to produce a return equivalent to a much larger population of reflecting but nonresonant targets.

At pressures greater than 1 atmosphere, the ratio of circumference to wavelength for a resonant bubble increases, providing the dimensions of the bubble do not change. This is because the resonant frequency shifts upwards, and may displace the entire resonant range of both the floats and extruded bubbles as observed in this study, beyond the 12 kc/s frequency employed in this work (table 13).

The following will illustrate these points. The resonant frequency of a bubble of radius, R , is generally written

$$f_r = \frac{1}{2\pi R} \left(\frac{3\gamma P_0}{\rho} \right)^{1/2} \quad (2)$$

where f_r is in cycles per second, R is in centimeters, γ = the ratio of specific heat of the gas in question at constant pressure to its specific heat at constant volume (which for air = 1.4 and for carbon monoxide also = 1.4), P_0 is the static pressure of the gas within the bubble in dynes/cm², and ρ = the specific gravity of the medium; in this case seawater = 1.025 gm/cm³.

For added ease in computation, equation 2 may be reduced to the approximate equation

$$f_r = \frac{(d+10)^{1/2}}{R} \quad (3)$$

where f_r is in kc/s, d is the depth in meters, and the radius, R , is in mm.

To determine the scattering cross section σ_s , of a bubble of radius R cm,

$$\sigma_s = \frac{4\pi R^2}{\left(\frac{f^2}{f_r^2} - 1 \right)^2 + \eta^2} \quad (4)$$

where f_r is the resonant frequency determined by equation 2 and f is the frequency actually employed. η is the ratio of circumference to wavelength and is given by

$$\eta = \frac{2\pi R}{\lambda} \quad (5)$$

in which the wavelength, λ , of the frequency in use is in centimeters. It is readily apparent that as f approaches f_r , the total

denominator in equation 4 becomes quite small and the resulting scattering cross section increases greatly. As an illustration, the bubble in Box 1, table 13, at 100 m would resonate at 58 kc/s. Its scattering cross section, σ_s , at 12 kc/s is very small, approximately $8 \times 10^{-6} \text{ cm}^2$, and the ratio of σ_s to the physical cross section is about 8×10^{-3} . It is thus relatively invisible to sonar at 12 kc/s. On the other hand, at the same depth the bubble shown in Box 3, table 13, would resonate at 12 to 13 kc/s and possess a σ_s of about 49 cm^2 . The ratio, $\sigma_s/\pi R^2$ is approximately 2200 or more than 5 orders of magnitude greater than the first bubble. From the above equations and the values presented in table 13, it is apparent that for constant bubble size f_r becomes greater with increasing P_0 .

The existence of pressure within the pneumatophore greater than ambient will tend to shift resonant frequency somewhat higher. In a previous study¹⁸ the author performed a preliminary analysis upon a series of floats in an effort to determine whether the gas within the float was generally under somewhat higher pressure than externally. Results indicated that after taking into account possible errors in measurement, on the average the gas within the pneumatophore was under little or no excess pressure. However, extremes within the groups analyzed indicated that in some cases the gases might be under an additional one or more atmospheres pressure with no obvious accompanying ballooning of the float (see, however, the exceptional Float F, table 11). Apparently, the apical sphincter can constrict to the point that gas cannot be passed, even under pressure. Upon occasion the author has found it impossible to extrude gas through the apical pore even when applying considerable pressure to the float, but this situation is not the rule. In any case, an internal over-pressure of, for example, one additional atmosphere, would shift the resonant frequency (equations 2 and 3) of a sphere with a radius equal to 0.3 mm at a depth of 300 meters, from about 59 kc/s to 60 kc/s. At 100 meters f_r would shift from 35 to 36.5 kc/s.

Other features which must also be considered are the damping effects of thermal conduction and acoustic radiation, and to a lesser degree, viscosity and surface tension effects. These factors, treated theoretically by Devin⁴⁵ and experimentally by Andrews,⁴⁶ must be accounted for when attempting to evaluate σ_s for real bubbles, since at resonance they contribute to the departure from ideality. For example, when dealing with real bubbles,

η in equation 4 is replaced by δ , the damping factor, which at resonance has a value of 0.058 (see ref. 46) for $f_r = 12$ kc/s. In the example given above, the bubble from Box 3, table 13, will now have a σ_s approximately equal to 26 cm^2 and a ratio of scattering cross section to physical cross section of 1200 vs. 2200 obtained using η .

These damping factors have not been evaluated for a non-spherical gas phase in a quasi-gelatinous bag such as the physonectid pneumatophore. Further, the departure from spherical shape might be expected to have some effect. Thus, while the pneumatophore itself closely approximates a regular prolate spheroid, the bubbles emitted, if in the size range observed above, will mostly take on a flattened oblate shape as they rise (see ref. 1, p. 120). According to work performed by M. Steinberg (cited in ref. 47, p. 519) scattering by a prolate spheroid can be shown to have a resonant frequency which varies as $P_0^{1/2}$ as in the case of spheres, providing the size and shape of the spheroid remain constant. From the work of Strasberg⁴⁸ (fig. 23), it can be seen that the ratio of resonant frequencies for a spheroid compared to a sphere increases rather slowly as the ratio of major to minor axis of the spheroid increases. This work was performed upon oblate shaped bubbles but may hold as well for spheroids of other shapes. The figure shows that spheroids possessing the dimensions of the floats given in table 11 may be expected to resonate at frequencies from somewhat above 1 percent higher to a maximum of about 10 percent higher than the resonant frequencies of spheres of equal volume. It is conceivable, however, that the presence of the float tissues may provide a damping effect which could offset this tendency toward upward shift in resonant frequency.

Further studies conducted by Lebedeva⁴⁹ showed the bulk modulus of elasticity for the tissues of various marine and freshwater fishes to differ only slightly from that of water, but the presence of a gas-filled swim bladder resulted in pronounced damping of the 0.9-kc/s sound employed, and a large reduction in the bulk modulus. The same author also experimentally determined a factor which she terms the dynamic complex shear modulus,⁵⁰ which is the tendency for a tissue to vibrate in response to a plane (tangential) wave. Between 1.58 and 14.3 kc/s she found the tissue-shear modulus to be frequency dependent, but similar for different species of fish. The shear modulus

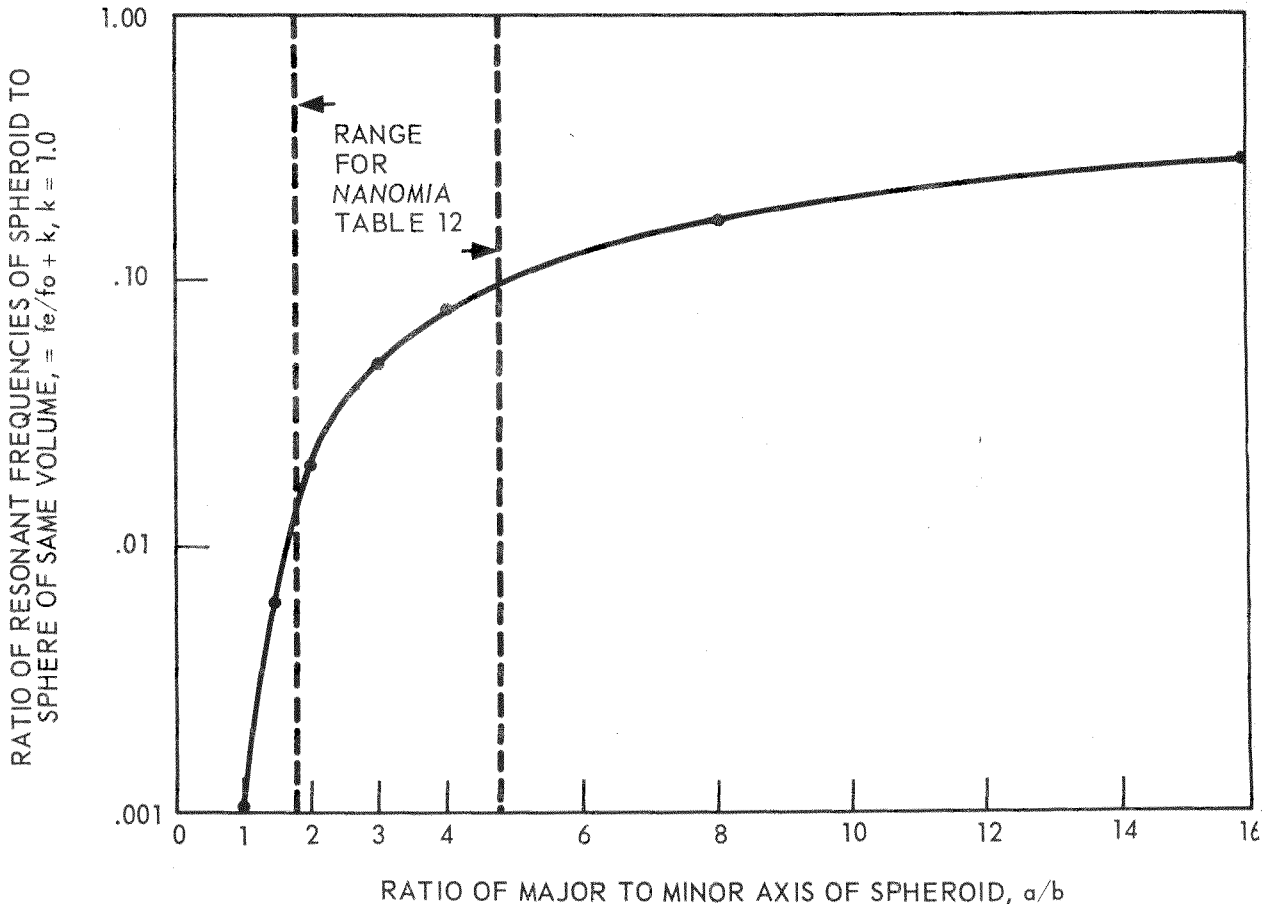


Figure 23. Ratio of resonant frequencies of a spheroid and a sphere plotted against the ratio of major to minor axis of the spheroid. Straight lines denote range in *Nanomia* dimensions. (Based on experimental data of Strasberg,⁴⁸).

tended to be greater at the higher frequencies and also greater when oriented perpendicular to the muscle fibers rather than longitudinally. These results are interpreted to imply that tangentially oriented sound waves may excite tissues to minor oscillations which might perform either a damping or enhancing function depending on amplitude and frequency when surrounding an acoustically active gas phase as in the siphonophore floats. The extent or significance of this possibility has yet to be evaluated, particularly for siphonophores.

However, Andreyeva and Chindonova⁵¹ employ the values obtained by Lebedeva to give the shear modulus, μ_0 , determined

exclusively for fish tissues, which was generally found to lie in the range 10^5 to 10^7 dynes/cm². They employ this in equation 2 to give

$$f_r = \frac{1}{2\pi R} \left(\frac{3\gamma P_0 + 4\mu_0}{\rho} \right)^{\frac{1}{2}} \quad (6)$$

which they then transform for convenience to the approximate form

$$f_r = 1.5 \sqrt{\frac{H+30}{V}} \quad (7)$$

where f_r is in kc/s, H , the depth in meters, and V , the volume of the gas bladder in mm³.

The significant difference between equations 3 and 7 is the fact that the former employs the radius of the bubble for which the minor semiaxis was substituted to obtain f_{ri} for pneumatophores in column $f_{ri(1)}$, table 13; whereas the latter equation employs the total volume of the gas phase. Thus values obtained by use of both equations, f_{ri} and f_{rs} , and by employing both the minor semiaxis and the radius of the sphere of equal volume for f_{ri} , are placed in table 13 for comparative purposes.

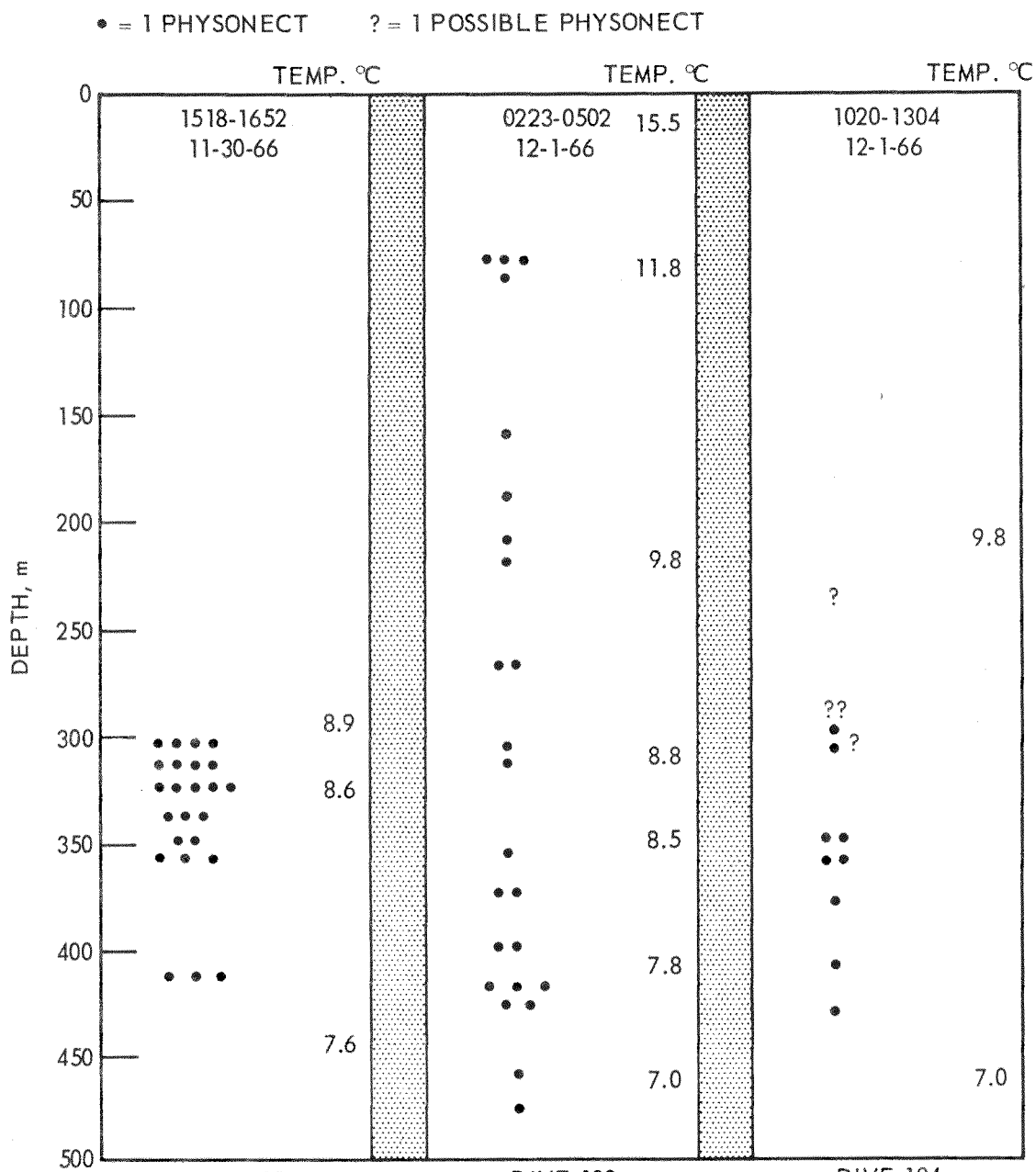
Although at this time the real value for μ_0 in the gelatinous tissues of siphonophores is unknown, it begins to appear that the volume, rather than some linear dimension, may be the most important aspect relative to resonance for a prolate spheroid. If this is true, then any significance ascribed to the continuous vertical orientation of the pneumatophore mentioned above disappears.

NUMBERS OF PHYSONECTID SIPHONOPHORES OBSERVED

Of fundamental importance to the foregoing is the number of siphonophores present in a given volume of water within the DSL particularly when it is coalesced at its daytime depth. This can now be assessed in two different ways -- by direct observation from deep submersibles and by net hauls. A number of difficulties accrue to both methods. In the case of direct observations from deep submersibles, the field of vision is limited by the geometry of the viewing ports to roughly a 90-degree arc.¹² The lights required for observation below the photic zone have varying effects on different species ranging from avoidance (negative phototaxis) through indifference to attraction (positive phototaxis). Thus, euphausiid shrimp sometimes literally swarm in the light fields of DEEPSTAR (observations on Dive 182); whereas, there is some evidence for light avoidance on the part of *Nanomia**^{12,52} In addition, the distance beyond the viewing port at which organisms can be seen and recognized depends on the number, intensity, and position of the lights in use, presence or absence of pigmentation on the animal, and rate of motion of the observer and the animal observed.

Bearing these limitations in mind, the author has computed the number of physonectid siphonophores observed during Dives 182 and 184 of DR/V DEEPSTAR 4000 (fig. 24 and table 1). These dives were undertaken during daylight hours when a single component DSL recorded on a Giff GDR-T was located at 310 to 365 meters (Dive 182) and 290 to 330 m (Dive 184). The dives were made with the lights on at all times while the vehicle descended slowly. By taking the conservative figure of 7 meters¹² as the greatest distance from the viewing port at which an animal could be recognized with certainty, and a 90-degree arc to represent total area under observation, a vertical wedge of water through the DSL from 300 to 450 meters equals a volume of roughly 5800 m³. In this vertical distance on Dive 182, 24 physonects were

*The author has seen nanomian siphonophores react to the flash of the DEEPSTAR strobe light by jerking abruptly and swimming down and away. They do not, however, characteristically respond to the gradual intrusion of the DEEPSTAR 1000-watt observation light in this way.



PHYSONECTID SIPHONOPHORES OBSERVED
DURING DIVES IN DR/V DEEPSTAR 4000

Figure 24. Number of physonectid siphonophores observed on three dives in DEEPSTAR 4000. For dive locations, see table 1.

seen making their density about $4/1000 \text{ m}^3$. Actually, the distribution of these siphonophores through the DSL strata was not uniform (fig. 24) so that at depths in the vicinity of 300 to 350 meters they appear to have been more abundant than this while toward the margins of the DSL they were less so. Thus, between 300 and 360 m the computed density is roughly 1 physonect per 100 m^3 . Dive 184, in an area of greater depth (table 1), produced fewer physonects at depths of the DSL to give a total of about 2 physonects/ 1000 m^3 between 300 and 430 meters by the above methods of reckoning.

By way of comparison, the heaviest collections of nanomian pneumatophores obtained by net hauls during a recent cruise gave densities of only about $0.5/1000 \text{ m}^3$ (table 14). The Tucker net^{6,20} used for these collections is constructed in such a way that there is no obstruction in the mouth of the net. However, a certain amount of net avoidance may have occurred during deep hauls when the heavy dredging cable used during this cruise might have sagged enough to hang down some distance in front of the net mouth. It is even more likely that the fragile colonies break up upon brushing the coarse mesh composing the sides of the fore-net and are swept out before reaching the nylon meter net and cod end bucket. Nanomians are well known to possess a high degree of autotomy.³¹

Although the distribution of these siphonophores is admittedly patchy in the vertical (fig. 24) as well as the temporal dimension, even within the DSL, and almost certainly to an equivalent or greater extent in the horizontal dimension, it is of some interest to estimate the total number that would be in the sound cone if the distribution across the diameter of the cone were uniform.

Thus, assuming an angle for the outgoing sonar of 30° , a truncated cone encompassing the DSL from 300 to 360 meters (fig. 24) would contain a volume of $1.5 \times 10^6 \text{ m}^3$ of seawater. Taking the DEEPSTAR observations for Dive 182 as representative of the entire truncated cone gives a total of 1.5×10^4 physonects for the entire sound field between these depths. For Dive 184 between 300 and 430 meters depth (fig. 24), a truncated cone of $3.9 \times 10^6 \text{ m}^3$ can be calculated to contain 7.9×10^3 physonectid siphonophores. Of these, only a comparatively small percentage is likely to be in or near the resonance range for 12 kc/s sound (tables 11, 12, and 13). Larger collections of these organisms must be made before the magnitude of this fraction can be reliably assessed.

TABLE 14. PHYSONECTID SIPHONOPHORE CATCH BY
TUCKER NET, OPERATION SIPHONOPHORE XI.

Net Haul Number	Avg. Drag Speed (knots)	Total Drag Time	Time at Depth of DSL (min)	Total Water Filtered at Depth of DSL (m^3)	Target DSL Centered at Depth (m)	Depth of Haul-Pinger* (m)	Depth of Haul-Depth Bomb** (m)	Total Physonects Captured†	Physonects per 1000 m^3 (approx.)
2 10-3-66	4.0	1626-1818	85	4.08×10^4	Beginning ascent from 330	190-220	220	19	0.5
3 10-3-66	4.5	1932-2050	57	3.13×10^4	Ascended layer 50 - 100	64	75-80	15	0.5
12 10-6-66	4.5	0755-0910	50	2.74×10^4	256	253-263		15	0.6

*Benthos Model No. 1020.

**Benthos Model No. 1170.

†Pneumatophores only counted.

The above figures are small, however, when compared with the maxima observed by Barham⁹ in the same area as that in which Dives 182 and 183 were made. Thus, his observations give between 100 and 300 nanomians/1000 m³ based on estimates made during Dive 113 in the bathyscaphe TRIESTE I, in October 1962. During the latter dive, unusually high-volume scattering measurements were recorded by Batzler¹¹ from a surface ship, from the exact level of Barham's coincident observations of the *Nanomia* layer. Peak values reported were -48 to -55 dB from a level where only sergestid prawns other than nanomian physonect siphonophores were observed. Taking Barham's most conservative estimate, 1 physonect/10 m³, gives a total of 4×10^5 siphonophores in a truncated sound cone between 280 and 420 meters depth, a water volume of 4×10^6 m³.

DISCUSSION

Oxygen Consumption And Carbon Monoxide Production

Significant aspects regarding the measurements and results for oxygen utilization and production of CO are that changing pH with changing pCO₂ might be expected to have had some effect on the respiratory and possibly the gas secretory apparatus of the live siphonophore float, but results from the syringe method, where the possibility arose, do not clearly indicate this. Thus, the lower values for syringe oxygen consumption from table 2 are in general comparable to those obtained by microrespirometer (tables 8 and 9). On the other hand, the higher values agree well with the lower values obtained by micrometer respirometer (table 10). In both this and the microrespirometer,³⁸⁻⁴⁰ no appreciable buildup of CO₂ with ensuing change in pH can occur.

There is still the problem of declining O₂ and increasing external CO. But, again, no clear-cut tendencies appear which would indicate that either factor was generally critical. It seems, therefore, that whatever effects these four factors (pH, pCO₂,

pO_2 , and pCO) may have exerted are obscured by the broad range in experimental conditions and results.

The possibility exists that CO may not become inhibitory to float tissues under ordinary circumstances. Thus, Larimer and Ashby²⁷ were unable to obtain inhibition of respiration in minced *Physalia* tissues by CO unless the available oxygen was reduced to about 5 percent. The same authors, however, found standard respiratory inhibitors such as cyanide (CN^-) and azide (N_3^-) to be very effective. They concluded that although a cytochrome system was surely present in the *Physalia* tissues which are ordinarily exposed to CO, the usual affinity of CO for cytochrome oxidase was not present at normal levels of pO_2 . It is interesting to note, however, that CO levels in *Nanomia* are three to five times as high as the highest values reported for *Physalia* and that oxygen, if present at all, is nearly always below 5 percent.¹⁶ This suggests the possibility that at least the cells in contact with the pneumatophore gas phase may have a unique means of meeting their respiratory demands. It is appropriate also to point out that newly secreted gas expelled as bubbles from the float seldom contains detectable O_2 or CO_2 (table 11). It is also pertinent to reiterate that at the depth of the DSL the pCO will be in the range of 30 to 45 atmospheres. At present we have little idea what special anatomy *Nanomia* and other physonects may possess for combating or accommodating to these partial pressures of a gas ordinarily lethal at a small fraction of the above values.

Variability in CO-producing capacity has been observed by Hahn and Copeland²⁸ in *Physalia*. Experiments conducted upon portions of the excised gas gland in syringes and with L-serine added at a concentration of 0.01M in all cases gave a maximum value for CO production of $1.75 \mu l/mg$ gas gland/hr and an average of $0.616 \mu l/mg$ g.g./hr at $22^\circ C$. These values drop to 0.780 and 0.438, respectively, under the influence of $65 \mu g/ml$ of aminopterin, a folic acid inhibitor. This further substantiates the study of Wittenberg and co-workers⁵³ who found *Physalia* gas glands to be rich in folic acid derivatives, and postulated that one of these acts as a carrier for the C_1 units derived from serine which ultimately appear as carbon monoxide gas.

By contrast, maximum results obtained from the present study for carbon monoxide production without bubble expulsion, when adjusted to $20^\circ C$ and equated on the basis of a gas gland equal to 10 percent of the pneumatophore weight (table 3), gave

4.50 μ l/mg gas gland/hr with L-serine added in 0.02M or 0.05M quantities, and 2.06 μ l/mg g.g./hr with no added substrate (table 2 and fig. 6). These are gas production rates obtained from intact gas glands within intact pneumatophores which have been broken off from the remainder of the colony during collection. Gas secretion rates increase strikingly in conjunction with bubble expulsion however, to rates when adjusted as above, that range from 15.5 to 115 μ l/mg g.g./hr for pneumatophores without added substrate and 277 for one float with serine added (table 11). Although the concentration of active enzyme in the minute gas gland is not known at present, it seems reasonable to surmise that the above rates are comparable to at least some of the slower of the known enzymatic reaction velocities.

Acoustics

Assumptions on production of bubbles at depth have, for the most part, been based on extrapolations from observations made on fresh-caught material at the surface (fig. 17 and 18). It is beyond the scope of the present study to discuss the various factors affecting bubble lifetimes at 300 to 400 meters in the sea. It can be said, however, that the diffusion gradient for carbon monoxide of 30 to 40 atmospheres will be the predominant factor, besides initial bubble size, which governs whether the bubble's tendency to dissolve will surpass its tendency to expand as it rises, or the reverse.

McCartney and Bary⁵⁴ have presented convincing evidence that rising bubbles produced in the bottom sediments of Saanich Inlet, British Columbia, were recorded on echo sounders. A number of intriguing questions arise from their observations, however, not the least of which is how a bubble of highly soluble H₂S originating at a depth of nearly 200 meters, and possessing a partial pressure of about 20 atmospheres, could survive across the vertical distance to depths of 30 meters as some of the presumed bubble tracks clearly show in the PDR records of these authors. The same holds true to a lesser degree for the less soluble CH₄, the only other prime candidate for a gas arising from anaerobic sediments. It is probable that our knowledge of diffusivities of these gases in water, and particularly seawater,

is still inadequate in terms of rising bubbles of various dimensions and velocities. An interesting experiment yet to be attempted with bubble traces specifically in mind, would be to anchor in deep water at sea and observe a rising DSL with high-resolution sonar in an effort to detect the bubbles given off by migrating siphonophores. When their ship was under way at speeds in excess of 3 to 5 knots, the above authors were not always able to differentiate their bubble traces from similar echoes presumed to be from fishes. Most scattering-layer research conducted at NEL to date has been aboard moving ships so that even were bubbles present in some quantity, they would appear on a PDR echogram to be small echo groups (termed SEG's — E.G. Barham, personal communication, and references 13, 55).

Finally, it is pertinent to consider the results obtained by Hersey and colleagues⁸ in a study of sound-scattering spectra from DSL's in the North Atlantic. These authors identified three layers on the basis of peak frequencies of scattered sound obtained from them. These layers were characterized by frequency ranges of 15 to 25 kc/s ("high frequency"), 6 to 11 kc/s ("intermediate frequency"), and about 2.5 to 5 kc/s ("low frequency"). Perhaps the most interesting feature of this study was the observation that during the migration of these layers the high-frequency layer displayed a frequency shift which varied as the 5/6th power of depth, while that of the intermediate-frequency layer varied as the 1/2 power of the depth. This was interpreted to imply that the high-frequency layer was composed largely of fishes which were neutrally buoyant only in the upper reaches of their migratory range and during migration their swim bladders contracted or expanded with changing hydrostatic pressure. In the case of the intermediate-frequency layers it was assumed that fishes within these layers were able to maintain buoyancy during migration.

On the basis of recent work in this laboratory by Capen⁵⁶ in which it was shown that the young of two species of lantern fish (Myctophidae) previously thought to have so-called "fat invested" swim bladders, in fact possess a small gas phase, it seems possible that one important contributor to the 5/6th power migratory layer may be myctophids. However, it is important to consider the possibility that, to some extent at least, physonectid pneumatophores may behave as Float F (table 11). If the pneumatophores tolerate expansion and contraction to this degree while

migrating, then within limits they may be expected to contribute to 5/6th power scattering. It is important to note that peak frequencies from this layer more closely approach hypothetical resonant frequencies for the majority of siphonophore floats and their released bubbles than is the case at 12 kc/s (table 13, figs. 20 and 21). However, for physonectid siphonophores which vent or resecrete gas to maintain approximate neutral buoyancy, peak frequencies will shift as the 1/2 power of depth. Large physonectids behaving in this matter would contribute to the intermediate layer of Hersey *et al.*

Further, in one of the most important pertinent studies made during World War II (ref. 44, p. 282-289) a deep scattering layer (or layers) was detectable at six stations covering a distance of 210 nautical miles on a transect from San Diego to Guadalupe Island, Mexico. These observations, made during January and February, 1943, were performed at 10, 20, 40, and 80 kc/s, and at each frequency a DSL was recorded. The possibility thus arises that a resonance peak will be observed in scattering at virtually any frequency in the range of about 10 to 100 kc/s, as shown in table 13, when a population of physonectid siphonophores of mixed age groups¹² is present. Because of possible variabilities in behavior, some of this population may produce peak resonance which varies as the 5/6th (or higher?) power of the depth while another part may vary as the 1/2 power of the depth.

On the basis of information presented in table 13 and figure 21, it is apparent that the majority of nanomian pneumatophores and their released bubbles thus far observed would be resonant at frequencies higher than 12 kc/s. However, the largest voluntary bubbles measured might be resonant at this frequency at depths of 100 meters, while the largest float-gas phases measured might be resonant to depths of nearly 400 meters. It cannot yet be said what proportion of the total physonect siphonophore population contributes to resonant scattering by the DSL, but it is important to note that the observed volume range of the floats alone covers a theoretical range in resonance from frequencies of less than 10 kc/s to 50 kc/s at depths from 100 to 400 meters.

SUMMARY

1. Carbon monoxide production by *Nanomia bijuga* showed rates, when not associated with bubble expulsion, reaching maxima of $2.06 \mu\text{l}/\text{mg}$ gas gland/hour at 20°C for pneumatophores not supplied with substrate for gas production, and $4.50 \mu\text{l}/\text{mg}$ g.g./hr when L-serine was added in 0.02 to 0.05 M quantities.

2. Levels of oxygen consumption not associated with carbon monoxide production were obtained from specimens of *Physalia*, *Velella*, and *Porpita*, and were generally in the range of 0.004 to $0.022 \mu\text{l}/\text{mg}$ whole animal/hr for the former species and 0.008 to $0.021 \mu\text{l}/\text{mg}$ /hr for the latter two species at 20°C .

3. Oxygen consumption determined by a syringe method, when associated with CO production, lay in the range 0.006 to $0.430 \mu\text{l}/\text{mg}$ /hr at 20°C for the intact nanomian pneumatophore and attached fragment of stolon. In general, oxygen consumption was distinctly elevated at higher rates of CO production.

4. Maximum observed values for oxygen consumption determined by an alternate method, when associated with CO production of undetermined extent, reached $0.860 \mu\text{l}/\text{mg}$ intact float/hr at 20°C .

5. Voluntary production of bubbles by the pneumatophores of *Nanomia bijuga* was observed and photographed, and measurements were made of the bubble volumes, rates of production and gas content.

6. Rates of carbon monoxide production deduced on the basis of bubble expulsion times reach values of 15.5 to $115 \mu\text{l}/\text{mg}$ gas gland/hr at 20°C when no substrate for gas production was present, and a maximum of $277 \mu\text{l}/\text{mg}$ g.g./hr in a single case where L-serine was added.

7. In two cases at about 22°C , pneumatophores lacking added substrate produced bubbles at a rate to equal their gas-phase volumes in 17 and 19 minutes, respectively, while a third pneumatophore with substrate added performed this function in only 13 minutes.

8. The revised range of observed gas-phase volumes for nanomian pneumatophores based on the present study is 0.25 mm^3 to 4.92 mm^3 with a single maximum to 12.56 mm^3 .

9. The observed range in volumes of voluntarily expelled bubbles is 0.03 mm^3 to 2.51 mm^3 with corresponding radii of about 0.18 mm and 0.85 mm , respectively.

10. Assuming these bubbles to be representative of the quantities of gas released during vertical migration and, therefore, of comparable volumes, the hypothetical range in resonance frequencies for depths of 100 to 400 meters will be 58 to 111 kc/s for the smaller, and 12 to 24 kc/s for the larger.

11. Direct observations from the deep submersible, DR/V DEEPSTAR, have indicated that nanomian pneumatophores are inflated at all times including morning hours. The pneumatophore is thus buoyant and was observed to orient vertically even when the siphonophore is swimming downward.

12. Hypothetical resonant frequencies for the pneumatophore calculated using the minor semiaxis as radius, from the two extremes given in paragraph 8 for depths of 100 to 400 meters, would be 42 to 81 kc/s, and 9 to 17 kc/s, respectively.

13. On the other hand, if the total volume, regardless of shape, is regarded as the most important aspect for resonance, the above values become 27 to 50 kc/s for the smaller float, and 7 to 13 kc/s for the larger.

14. Although in a previous report little evidence for internal over-pressure in the float was found, on the average, a few values suggested the possibility of internal pressures above ambient of perhaps one atmosphere, or slightly more, with little or no indication of stretching or ballooning in the pneumatophore. In the present work, a volume increase caused by stretching of the float walls was observed, in a single instance amounting to a little over four times.

15. Deep scattering layers were recorded on a Gifft GDR-T when the computed number of pneumatophore-bearing siphonophores in a truncated sound cone encompassing the DSL, based upon direct observations, was as low as 2 siphonophores/1000 m³. Of these, only a small percentage might have been resonant to the 12-kc/s sonar in use. The fractional contribution to scattering from other potential scatterers within this DSL as well as from the siphonophores is yet to be determined.

RECOMMENDATIONS

1. Further determine gas-secreting capabilities of siphonophore floats and particularly of excised gas glands.
2. Determine the effects of pressure on these capabilities and on volumes of released bubbles.
3. Study the behavior of bubbles of pure gas in sound fields and when rising in tubes.
4. Determine diffusion characteristics of pertinent types of gas bubbles; include pressure effects.
5. Relate 3 and 4 (above) in an effort to formulate a predictive framework for bubble lifetimes.
6. Attempt open-sea observations for bubbles associated with the deep scattering layer.
7. Measure target strength of the inflated pneumatophore, and determine scattering cross sections and the effects of shear and other damping or enhancing factors at resonance.

APPENDIX A: PROCEDURE FOLLOWED IN SYRINGE RESPIROMETRY AND GAS PRODUCTION EXPERIMENTS

1. Select pneumatophore specimen and measure under dissecting microscope employing an ocular micrometer.
2. Gently expel small bubble from pneumatophore into a micro gas reservoir charged with acidified, saturated sodium citrate.
3. Remeasure float and place in syringe with drop of mercury for stirring. Take care to trap no air in syringe.
4. Place specimen syringe together with identical control syringe lacking a specimen in refrigerator or water bath. Note time.
5. Analyze extruded bubble (fig. 3 in main text).
6. Perform analyses on stock seawater and perform reagent blank determinations as required. Periodically note experimental temperature and record barometric pressure.
7. After desired length of time, remove experimental and control syringes and again note time.
8. Carefully expel water sample (using a calibrated safety spacer on syringe plunger) from experimental syringe into extractor syringe for analysis of dissolved gases²².
9. Gently remove float from syringe and measure.
10. Expel all gas from float and measure volume of expelled gas either in a calibrated capillary tube or by using an ocular micrometer and pipette, or, occasionally both.
11. Analyze expelled gas.

12. Analyze water sample held in extractor syringe for dissolved gases.

13. Similarly, analyze water in control syringe.

Calculations

Let the dissolved O₂ in syringe water at the start (stock) plus any O₂ in the float at start equal the total available O₂ at the start of the experiment, V_s, and the dissolved O₂ in the syringe water at the end plus any O₂ in the float at the end, V_e, while the dissolved O₂ at the start (stock) minus the dissolved O₂ at the end in the control syringe equals the control O₂ consumed, C, all analyses corrected for reagent blanks. Then the total volume of dry oxygen consumed at standard conditions, V₀, is given by

$$V_0 = \frac{(V_s - V_e - C) P}{760} \cdot \frac{273}{273 + T}$$

where P = barometric pressure corrected for water vapor pressure and for additional factors depending on type of barometer employed, and T is the experimental temperature in °C.

A similar procedure is followed when determining the amount of carbon monoxide evolved.

APPENDIX B: EXPERIMENTAL ERRORS AND ACCURACY OF MEASUREMENTS

Syringe Method

At best, under typical operating conditions at sea, the analyzer for dissolved oxygen²² can give results for duplicate analyses within ± 0.2 to $\pm 0.3 \text{ mm}^3$. These values incorporate errors arising from sample transfer to the extractor syringe as well as extractor reagent errors and errors in the analyses of the extracted gas.*

Thus, using Float F, table 2, as an example: after correction for reagent blanks and controls, the amount of oxygen consumed was 3.8 mm^3 . Allowing for an error in the first and last reading of $\pm 0.3 \text{ mm}^3$, a maximum value would become 4.4 mm^3 and a minimum 3.2 . That is, the maximum would be obtained when the first volume measurement was read $+0.3 \text{ mm}^3$ and the final volume measurement was read -0.3 mm^3 . The minimum value would be obtained by doing the reverse for each volume reading. The difference between these values, 1.2 mm^3 when divided by the total time of the experiment, 769 minutes, equals about 0.002 mm^3 oxygen consumed/min or $0.120 \text{ mm}^3/\text{hr}$. When divided by the total weight of the specimen, 8.8 mg , this becomes $0.014 \text{ mm}^3/\text{mg}/\text{hr}$, or an error of $\pm 0.007 \text{ mm}^3/\text{mg}/\text{hr}$.

It is apparent that this error will vary somewhat for each experiment depending on total experiment time and total weight of the individual specimen. This holds true also for the determination of dissolved carbon monoxide, but duplicate analyses for this gas generally agree within 0 to 0.2 mm^3 . The corresponding error for Float F, for example would become ± 0.002 to $\pm 0.004 \text{ mm}^3/\text{mg}/\text{hr}$ for CO.

*See ref. 18, Appendix A, and the original paper (ref. 22) for a discussion of the use of this analyzer for straight gas analysis.

Pipette Analysis

The ocular micrometer at the magnification used could be read to about ± 0.03 mm. This would give rise to an error in volume estimates of approximately ± 0.007 mm³ for a bubble of 0.032 mm³, ± 0.024 mm³ for a bubble of 0.214 mm³, and ± 0.12 mm³ for a bubble of 2.14 mm³. The above values are given as examples and also approximate the volume range of voluntarily expelled bubbles given in table 13 in the main text.

Microrespirometer

The volume displacement of the drill rod, which by vertical position indicates oxygen consumption in this instrument, can be read with a vernier scale to ± 0.73 mm³. In the case of *Physalia* (see table 8 in the main text) with an experiment time of 282 minutes and a weight of 100 mg, for example, this is equivalent to an error of about ± 0.002 mm³/mg/hr. In the original paper describing this method,³⁸ the reading error is indicated to be about 1 mm³/hr which then equals by the above treatment an error of about ± 0.005 mm³/mg/hr.

Micrometer Respirometer

The 1/16th-inch drill rod in this instrument⁴⁰ displaces 1.96 mm³ for each millimeter of travel. The micrometer has 100 divisions per millimeter and each division can be read to ± 0.2 to ± 0.3 with a hand lens. This is equivalent to a reading error of ± 0.004 to ± 0.007 mm³.*

*Note that in this report cubic millimeters, mm³, and microliters, μ l, are taken as being equivalent.

APPENDIX C: EXTERNAL PNEUMATOPHORE DIMENSIONS

To clarify the dimensions given for the internal gas phase of the pneumatophores listed in table 2 in the main text, the external dimensions of the same floats are listed in table C-1. Dimension changes indicated are associated with bubble production (see table 11).

TABLE C-1. EXTERNAL DIMENSIONS OF PNEUMATOPHORES

Float	Length* (mm)	Width (mm)	Float	Length (mm)	Width (mm)	Float	Length (mm)	Width (mm)
O	3.75	1.38	A	2.87	0.75	B	a)4.75	1.38
D	2.75	0.75	G	4.38	1.13		b)4.63	1.25
C	a)3.50 b)4.13	1.25 1.00	H	5.25	1.38	U	2.63	1.00
N	a)3.50 b)3.75	1.38 1.63	R	2.88	1.25	T	3.13	0.88
J	5.00	1.50	Q	3.63	1.25	S	2.75	1.00
L	3.13	1.13	F	a)5.63 b)5.25 c)4.88	1.50 2.63 2.25	E	4.38	1.50
K	3.50	1.13	P	4.38	1.88	(E, gas phase)	3.62	1.25
I	3.75	1.00	M	a)4.13 b)4.13	1.00 1.25			

*More than one set of measurements indicates a change in dimensions resulting from bubble expulsion. Compare with corresponding gas phase dimensions given in table 11 (in main text).

APPENDIX D: DIFFUSION CONDITIONS FOR SYRINGE EXPERIMENTS*

Figure D1 presents three hypothetical graphs depicting alternate possibilities for the time sequence of diffusion of carbon monoxide gas from the pneumatophore to the seawater relative to production of the same gas by the float gas gland. One or another of these alternatives can be invoked to explain the quantities of gas actually measured during an experiment from within the float and dissolved in the surrounding seawater.

"Maintenance rates" vary with percent CO maintained since higher diffusion gradients diffuse relatively more CO. Thus, for 80 to 90 percent CO within the pneumatophore, maintenance rates must be quite high. Also, oxygen consumption will increase with increasing CO production simply for maintenance purposes.

Those floats with greater diffusion than production presumably began with high gradients which diffused large amounts of CO into the seawater, but did not maintain production at rates sufficient to retain those levels within the float. In this case, most of the CO was in the water by the end of the run. With the exception of float N, these are mostly the shorter runs.

Note that those which appear to have produced more CO than was diffused, have relatively higher percent CO in the float at the end of the experiment than at the start. The reverse seems to be true for those with what appears to be less CO produced than diffused. Floats O* and B approach a true maintenance rate where percent CO at start is approximately equal to percent CO at the end. ** Not surprisingly, those experiments run at high temperatures fulfill figure D1-A condition while most run at low temperatures appear to meet the D1-B condition.

*An asterisk by a float letter denotes an experiment with serine added.

**Refer also to tables 5, 6, and 7 in the main text for pertinent information.

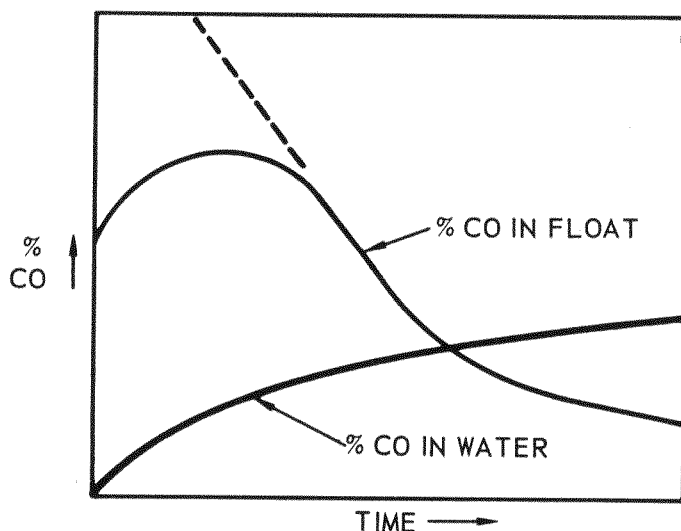


Figure D1. A. If ending percent CO in float is less than starting percent, as in this figure, then all additional CO produced will have diffused out of the float, plus the difference in starting and ending percent, multiplied by the float volume. The dashed line denotes the hypothetical curve if secretion had begun with the start of the experiment, or if the initial percentage of CO had been high with no subsequent secretion. This situation seems particularly true for the high-temperature runs such as M, U* and T*, also N*, probably R* and possibly P*. (See table 6 in main text).

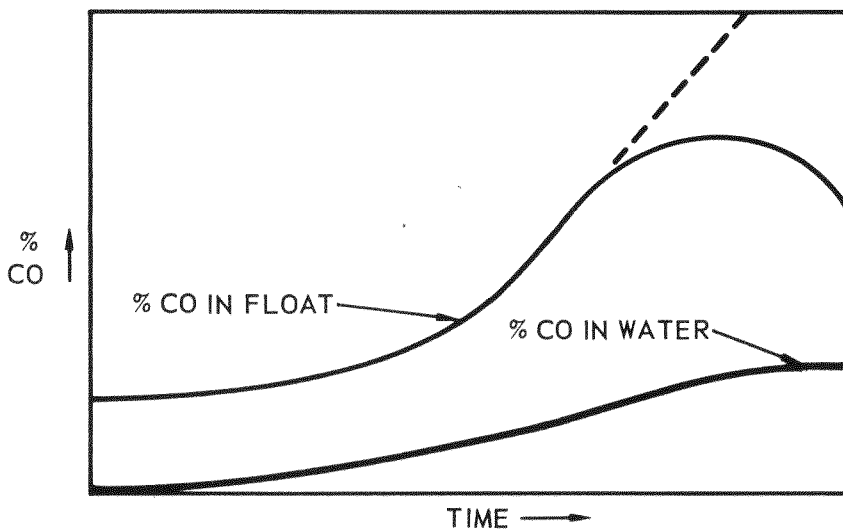


Figure D1. B. If ending percent CO in float is greater than starting percent, as in this figure, then production surpasses diffusion. That is, the amount produced did not have time to diffuse entirely away. This situation was probably true for floats F and H, and possibly floats O*, D, C, and to a slight extent, B.

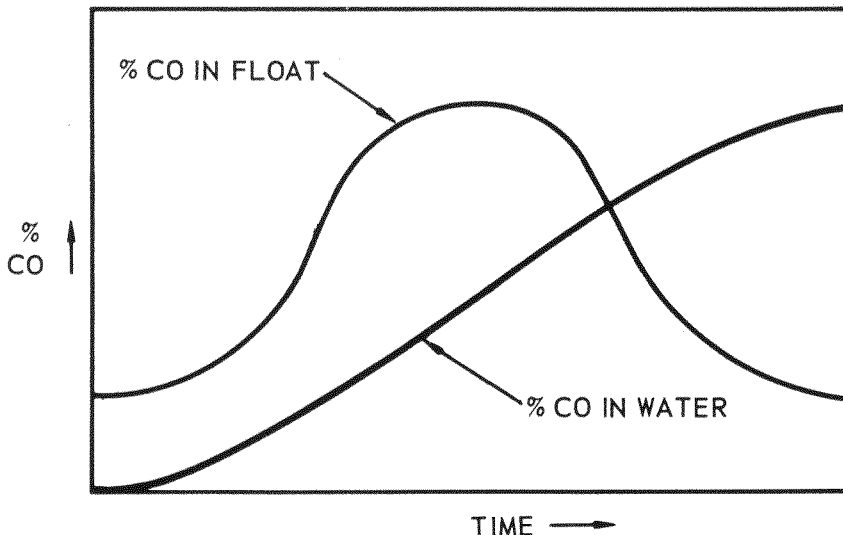


Figure D1. C. This figure represents the special case where starting and ending percentage of CO in the float is approximately the same:
a) The production burst may have occurred in the middle of the experimental period in which case the amount diffused may approximately equal the amount produced. Floats O* and B could conceivably represent this situation. b) Production may have metered along at about the same rate throughout the experiment and approximately equaled the diffusion rate so that at the end the final result would be the same.

APPENDIX E: ANALYSES OF FLOAT GASES FROM *PHYSALIA* AND *VELELLA*

The float gases from *Physalia*, the Portuguese Man-of-War, and from *Velella*, the Sail-by-the-Wind, were analyzed at the Lerner Marine Laboratory of the American Museum of Natural History on Bimini Island, Bahamas, in January and February 1962. Results of the analyses are presented in tables E-1 and E-2. Specimens were collected as indicated and gas samples were taken for analysis within a few hours of capture. Gas samples from *Physalia* were taken with greased syringes; those from *Velella* were taken with syringes charged with a saturated solution of acidified sodium citrate and using a small-gauge hypodermic needle. All *Velella* specimens were held under water while the gas sample was withdrawn.

At present the maximum published values for percentage of carbon monoxide in the float of *Physalia* are as follows: Wittenberg, 1960 (ref. 17), employing the gasometric technique of Scholander *et al.*,²² with a cuprous chloride in ammonium chloride solution (Winkler's Reagent) found values to 12.7 percent from 29 animals checked; very small quantities of CO were successfully detected by Wittenberg using the ultrasensitive palladium sulfate method of Shepherd;⁵⁷ Clark and Lane, 1961,³⁶ employing the very accurate Scholander 0.5 cc analyzer⁵⁸ and Winkler's reagent reported values to 6.07 percent from 12 animals analyzed; Larimer and Ashby, 1962,²⁷ found maxima to 20.8 percent using a gas chromatograph (32 analyses), and 19.3 percent using a mass spectrometer (14 analyses); Hahn and Copeland, 1966,²⁸ reported quantities to 28 percent (20 specimens); these authors also employed the method of Shepherd.⁵⁷

For the analyses reported in tables E-1 and E-2, the analyzer of Scholander, *et al.*²² was used together with Winkler's reagent as carbon monoxide absorber. To the best of the author's knowledge, these are the first such analyses reported for *Velella*.

TABLE E-1. ANALYSES OF FLOAT (PNEUMATOPHORE) GASES OF *PHYSALIA*
 (Bimini, Bahamas, Jan-Feb 1962)*

Species	Specimen No.	Float Length (mm)	CO ₂ (%)	O ₂ (%)	CO (%)	N ₂ (%) **
<i>Physalia physalis</i>	1	30	0.9	15.2	4.4	79.5
	2	33	1.6	13.8	2.0	82.6
	3	35	1.2	14.0	7.1	77.7
	4	48	0.9	17.5	0.4	81.2
	5	60	1.5	15.2	5.2	78.1
	6	65	1.5	16.3	4.2	78.0
	7	75	2.7	15.7	5.2	76.4
	8	75	0.5	8.2	16.0	75.3
	9	90	0.8	17.2	6.1	75.9
	10	100	1.0	16.1	7.0	75.9
	11	110	1.7	14.5	10.5	73.3
	12	110	1.1	14.2	9.6	75.1
	13	150	1.1	13.1	16.9	69.9
	14	180	1.0	16.5	5.4	77.2
	15	200	0.1	18.1	2.6	79.2
	16	200	1.1	17.9	5.5	76.1

*All specimens collected while still afloat, i.e., before stranding.

**Obtained by difference.

TABLE E-2. ANALYSES OF FLOAT (PNEUMATOPHORE) GASES OF VELELLA
(Bimini, Bahamas, Jan-Feb 1962)

	No.	CO ₂ (%)	O ₂ (%)	N ₂ * (%)	Remarks
<i>Velella velella</i>	1	0.9 **	ND	99.1	Specimens collected freshly washed ashore.
	2	ND	1.4	98.6	
	3	ND	2.5	97.5	
	4	ND	20.0	80.0	
	5	ND	2.5	97.5	
	6	2.5	16.9	80.6	
	7	2.4	9.9	87.7	Specimens collected while still afloat.
	8	3.2	3.8	92.9	
	9	2.4	1.2	96.4	
	10	3.7	2.7	93.5	
	11	3.0	3.8	93.1	
	12	2.1	2.6	95.3	
	13	3.0	5.6	91.4	

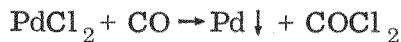
*N₂ obtained by difference. CO in all cases absent.

**ND = Not detectable.

APPENDIX F: NOTE REGARDING CONFIRMATORY ANALYSES FOR CARBON MONOXIDE

Although not published heretofore, early in the study of the physiology of siphonophores from the DSL a few confirmatory analyses for CO employing a different reagent were carried out. While Winkler's reagent is an excellent absorber for CO, it will also absorb a number of other gases, if present, such as O₂ and CO₂.⁵⁹ Routinely, the latter gases are absorbed from any sample undergoing analysis before the Winkler's reagent is employed. However, the possibility of other contaminants should be ruled out by confirmatory analyses using different reagents. Thus, Wittenberg¹⁷ used the Winkler's solution for the most part in analyses of *Physalia* gases for CO, but confirmed the nature of the gas by using Shepherd's PdSO₄ method⁵⁷ and further confirmed the gas by its characteristic spectrum when equilibrated with hemoglobin solutions to give carboxy hemoglobin.

When dealing with *Nanomia* gases, in a number of cases freshly caught and intact pneumatophores were floated in a solution of 1/200th N palladium chloride in the center well of a sealed Conway dish.⁴¹ Within a short period the entire external surface of the floats was black with the precipitated palladium confirming the diffusive nature of the entire pneumatophore epithelium and the character of the gas according to the reaction:⁶⁰



which continues



Formalized floats possessing a gas phase which have been preserved for periods of 4 to 5 months do not produce a black precipitate by the above method even after 24 hours in PdCl₂.

A number of analyses were performed on a routine basis employing palladium chloride as CO absorber in place of Winkler's reagent with entirely comparable and satisfactory results.

REFERENCES

1. National Defense Research Committee. Division 6 Summary Technical Report, v. 7, Principles and Applications of Underwater Sound, p.100-102, 1946
2. Johnson, M.W., "Sound as a Tool in Marine Ecology, From Data on Biological Noises and the Deep Scattering Layer," Journal of Marine Research, v.7, p.443-458, 1948
3. Dietz, R.S., "Deep Scattering Layer in the Pacific and Antarctic Oceans," Journal of Marine Research, v.7, p.430-442, 1948
4. Raitt, R.W., "Sound Scatterers in the Sea," Journal of Marine Research, v.7, p. 393-409, 1948
5. Marshall, N.B., "Bathypelagic Fishes as Sound Scatterers in the Ocean," Journal of Marine Research, v.10, p.1-17, 1951
6. Tucker, G.H., "Relation of Fishes and Other Organisms to the Scattering of Underwater Sound," Journal of Marine Research, v.10, p.215-238, 1951
7. Hersey, J.B. and Backus, R.H., "New Evidence That Migrating Gas Bubbles, Probably the Swim Bladders of Fish, are Largely Responsible for Scattering Layers on the Continental Rise South of New England," Deep-Sea Research, v.1, p.190-191, 1954
8. Hersey, J.B. and others, "Sound-Scattering Spectra of Deep Scattering Layers in the Western North Atlantic Ocean," Deep-Sea Research, v.8, p.196-210, 1962
9. Barham, E.G., "Siphonophores and the Deep Scattering Layer," Science, v.140, p.826-828, 17 May 1963
10. Barham, E.G., "The Deep Scattering Layer as Observed From the Bathyscaphe TRIESTE (Abstract)," p.298-300 in International Congress of Zoology, Proceedings, 16th, v.4, 20-27 August 1963, XVI International Congress of Zoology, 1963

11. Batzler, W.E. and Barham, E.G., "Acoustic Scattering From a Layer of Siphonophores (Abstract)," Acoustical Society of America. Journal, v.35, p.792-793, May 1963
12. Barham, E.G., 'Deep Scattering Layer Migration and Composition: Observations From a Diving Saucer,' Science, v.151, p.1399-1403, 18 March 1966
13. Barham, E.G. and Davies, I.E., "Bio-Acoustics," p.31-38 in Navy Electronics Laboratory, NEL Deep Submergence Log No. 1, August 1966
14. Barham, E.G., Davies, I. E. and Wilton, J.W., "Bio-Acoustics," p.15-26 in Navy Electronics Laboratory, NEL Deep Submergence Log No. 2, October 1966.
15. Davies, I. E., Barham, E.G. and Pickwell, G.V., "Bio-Acoustics," p.47-52 in Navy Electronics Laboratory, NEL Deep Submergence Log No. 3, February 1967
16. Pickwell, G.V., Barham, E.G. and Wilton J.W., "Carbon Monoxide Production by a Bathypelagic Siphonophore," Science, v.144, p.860-862, 15 May 1964
17. Wittenberg, J.B., "The Source of Carbon Monoxide in the Float of the Portuguese Man-of-War, *Physalia physalis* L.," Journal of Experimental Biology, v.37, p.698-705, 1960
18. Navy Electronics Laboratory Report 1369, Physiological Dynamics of Siphonophores From Deep Scattering Layers, by G.V. Pickwell, 20 April 1966
19. Mackie, G.O., "Studies on *Physalia physalis* (L.), Part 2: Behaviour and Histology," Discovery Reports, v.30, p.371-407, November 1960
20. Davies, I. E. and Barham, E.G., "An Automatic Opening-Closing Net for Collection of Mid-Depth Organisms, Particularly in the Deep Scattering Layer" (In preparation)

21. Arthur, R.S., "Variation in Sea Temperature Off La Jolla," Journal of Geophysical Research, v. 65, p. 4081-4086, December 1960
22. Scholander, P.F. and others, "Micro Gasometric Determination of Dissolved Oxygen and Nitrogen," Biological Bulletin, v. 109, p. 328-334, 1955
23. Tang, P.S., "On the Rate of Oxygen Consumption by Tissues and Lower Organisms as a Function of Oxygen Tension," Quarterly Review of Biology, v. 8, p. 260-274, 1933
24. Giese, A.C., Cell Physiology, 2d ed., p. 200-204, W.B. Saunders, 1962
25. Jacobs, W., "Beobachtungen über das Schweben der Siphonophoren," Zeitschrift für Vergleichende Physiologie, v. 24, p. 583-601, 1937
26. Jacobs, W., "Floaters of the Sea," Natural History, v. 71, p. 23-27, August-September 1962
27. Larimer, J.L. and Ashby, E.A., "Float Gases, Gas Secretion and Tissue Respiration in the Portuguese Man-of-War, *Physalia*," Journal of Cellular and Comparative Physiology, v. 60, p. 41-47, August 1962
28. Hahn, W.E. and Copeland, D.E., "Carbon Monoxide Concentrations and the Effect of Aminopterin on Its Production in the Gas Bladder of *Physalia physalis*," Comparative Biochemistry and Physiology, v. 18, p. 201-207, May 1966
29. Lane, C.E., "Observations on the General Biology of *Physalia* (Abstract)," American Zoologist, v. 1, p. 367, August 1961
30. Miami University Institute of Marine Science, Marine Laboratory Contract Nonr 840 (17); Final Report, General Biology of *Physalia*, by C.E. Lane, September 1964

31. Mackie, G.O. and Boag, D.A., "Fishing, Feeding and Digestion in Siphonophores," Naples. Stazione Zoologica. Pubblicazioni, v. 33, p. 178-196, 1963
32. Riley, G.A., "Organic Aggregates in Seawater and the Dynamics of Their Formation and Utilization," Limnology and Oceanography, v. 8, p. 372-381, October 1963
33. Ahlstrom, E.H. and Threlkill, J.R., "Plankton Volume Loss With Time of Preservation," California Cooperative Oceanic Fisheries Investigations, Reports, v. 9, p. 57-73, January 1963
34. Adams, R.L., "Bio-Acoustic Scattering Measurements," p. 53-56 in Navy Electronics Laboratory, NEL Deep Submergence Log No. 3, February 1967
35. Totton, A.K., "Siphonophora of the Indian Ocean, Together With Systematic and Biological Notes on Related Specimens From Other Oceans," Discovery Reports, v. 27, p. 1-162, April 1954
36. Clark, F.E. and Lane, C.E., "Composition of Float Gases of *Physalia physalis*," Society for Experimental Biology and Medicine. Proceedings, v. 107, p. 673-674, 1961
37. Hyman, L.H., The Invertebrates: Protozoa Through Ctenophora, p. 481, McGraw-Hill, 1940
38. Scholander, P.F. and others, "Microvolumetric Respirometry; Methods for Measuring O₂ Consumption and CO₂ Production by Cells and Enzymic Reactions," Journal of General Physiology, v. 35, p. 375-395, 20 January 1952
39. Scholander, P.F. and Iversen, O., "New Design of Volumetric Respirometer," Scandinavian Journal of Clinical and Laboratory Investigation, v. 10, p. 429-431, 1958
40. Scholander, P.F., "Volumetric Microrespirometers," Review of Scientific Instruments, v. 13, p. 32-33, January 1942
41. Conway, E.J., Microdiffusion Analysis and Volumetric Error, 4th rev. ed., p. 326-330, London: Lockwood, 1957

42. Chapman, D. J. and Tocher, R.D., "Occurrence and Production of Carbon Monoxide in Some Brown Algae," Canadian Journal of Botany, v.44, p.1438-1442, 1966
43. Midttun, L. and Hoff, I., "Measurements of the Reflection of Sound by Fish," Reports on Norwegian Fishery and Marine Investigations, v.13, No.3, p.4-18, 1962
44. National Defense Research Committee. Division 6 Summary Technical Report, v. 8, Physics of Sound in the Sea, 1946
45. Devin, C., Jr., "Survey of Thermal, Radiation, and Viscous Damping of Pulsating Air Bubbles in Water," Acoustical Society of America, Journal, v.31, p.1654-1667, December 1959
46. Andrews, D.E., Jr., Acoustic Properties of Individual Air Bubbles in Water, (Ph.D. Thesis, University of California at Los Angeles), 1960
47. Hersey, J.B. and Backus, R.H., "Sound Scattering by Marine Organisms," p.498-539 in Hill, M. N., The Sea; Ideas and Observations on Progress in the Study of the Seas, v.1: Physical Oceanography, Interscience, 1962
48. Strasberg, M., "The Pulsation Frequency of Nonspherical Gas Bubbles in Liquids," Acoustical Society of America. Journal, v.25, p.536-537, May 1953
49. Lebedeva, L.P., "Measurement of the Bulk Modulus of Elasticity of Animal Tissues," Soviet Physics: Acoustics, v.10, p.410-411, April-June 1965
50. Lebedeva, L.P. "Measurement of Dynamic Complex Shear Modulus of Animal Tissues," Soviet Physics: Acoustics, v.11, p.163-165, October-December 1965
51. Andreeva, I.B. and Chindonova, Y.G., "O Prirode Zvukorasseivaiushikh Sloev (On the Nature of Sound-Scattering Layers)," Okeanologiya, v.4, p.112-124, 1964

52. Mackie, G.O., "Pigment Effector Cells in a Cnidarian," Science, v.137, p.689-690, 31 August 1962
53. Wittenberg, J.B. and others, "Folic Acid Derivatives in the Gas Gland of *Physalia physalis* L.," Biochemical Journal, v.85, p.9-15, 1962
54. McCartney, R.S. and Bary, B.M., "Echo-Sounding on Probable Gas Bubbles From the Bottom of Saanich Inlet, British Columbia," Deep-Sea Research, v.12, p.285-294, June 1965
55. Navy Electronics Laboratory Report 1368, Marine Organisms as Spurious Acoustic Targets, by E.G. Barham and I.E. Davies, CONFIDENTIAL, 8 April 1966
56. Navy Electronics Laboratory Report 1447, Swimbladder Morphology of Some Bathypelagic Fishes in Relation to Sound Scattering, by R.L. Capen, 20 March 1967
57. Shepherd, M., "Rapid Determination of Small Amounts of Carbon Monoxide," Analytical Chemistry, v.19, p.77-81, February 1947
58. Scholander, P.F., "Analyzer for Accurate Estimation of Respiratory Gases in One-Half Cubic Centimeter Samples," Journal of Biological Chemistry, v.167, p.235-270, January 1947
59. Ambler, H.R., "On the Absorption of Carbon Monoxide, Part I: A Critical Comparison of Some Methods Employed in Gas Analysis," Analyst, v.50, p.167-174, 1925
60. Winkler, L.W., "Halbmikroverfahren zur Bestimmung des in die Luft gelangten Kohlenoxydes," Zeitschrift für Analytische Chemie, v.97, p.18-27, 1934